

NPS ARCHIVE
1963
SHAVER, W.

INVESTIGATIONS OF A TUNABLE
RADIO FREQUENCY RC BANDPASS FILTER
WILLIAM M. SHAVER

LIBRARY
U.S. NAVAL POSTGRADUATE SCHOOL
MONTEREY CALIFORNIA

INVESTIGATIONS OF A TUNABLE
RADIO FREQUENCY
RC BANDPASS FILTER

* * * *

WILLIAM M. SHAVER

INVESTIGATIONS OF A TUNABLE
RADIO FREQUENCY
RC BANDPASS FILTER

by

William M. Shaver

//
Lieutenant Commander, United States Navy

Submitted in partial fulfillment of
the requirements for the degree of

MASTER OF SCIENCE
IN
ENGINEERING ELECTRONICS

United States Naval Postgraduate School
Monterey, California

1 9 6 3

INVESTIGATIONS OF A TUNABLE

RADIO FREQUENCY

RC BANDPASS FILTER

by

William M. Shaver

This work is accepted as fulfilling
the thesis requirements for the degree of

MASTER OF SCIENCE

IN

ENGINEERING ELECTRONICS

from the

United States Naval Postgraduate School

ABSTRACT

The principles of operation of commutated filters have been known for sometime, however, very little work has been done in the development of these devices, particularly at radio frequencies. It would appear that this device might be useful in the current industry trend toward micro-miniaturization. The theory of operation of a commutated RC bandpass filter is discussed and a complete mathematical derivation is presented. Operating data on a complete, solid state radio frequency filter is given and extensively discussed. Finally, a new and different type of commutated filter employing the recently developed madistor is proposed.

The writer wishes to express his appreciation for the assistance and encouragement given him by Professors Clarence F. Klamm, Jr., Paul E. Cooper and William M. Bauer, of the United States Naval Postgraduate School and to Mr. Robert Anderson of the Office of Naval Research at the United States Naval Postgraduate School.

TABLE OF CONTENTS

Section	Title	Page
1.	Introduction	1
2.	The Sampled Data Bandpass Filter	3
	2-1 Low Pass Filter	3
	2-2 Synthesis of the Bandpass Filter	4
	2-3 General Comments on the Filter Characteristics	7
3.	A Practical Solid State RC Filter	10
	3-1 Switch Considerations	10
	3-2 Operation of the Digital Switch	10
	3-3 Discussion of Results Obtained from Operation of the Digital Switch	13
4.	An Alternate Approach with the Madistor	23
	4-1 The Madistor	23
	4-2 Employing the Madistor as a Stepping Switch	25
	4-3 Discussion and Summary of Madistor-Filter	27
5.	General Discussion Conclusion and Recommendations	28
6.	Bibliography	30
7.	Appendix A	31
8.	Appendix B	39

LIST OF ILLUSTRATIONS

Figure		Page
2-1	Low Pass Filter	3
2-2	Frequency Response	3
2-3	Translation of Low Pass Response	4
2-4	Schematic of Switching Commutator	5
2-5	Depiction of Sampling Pulses	6
2-6	Sketch of Transfer Function $H(f_c)$	8
3-1	Block Diagram for Digital Switch	11
3-2	Relationship of Switching Waveforms along with Schematic of One of Four Identical Bridges	11
3-3	Switching Sequence of Bridges	13
3-4	Switching Sequence Showing Defective Switching Action	14
3-5	Filter Response	19
3-6	Filter Response	20
3-7	Filter Response	21
3-8	Filter Response	22
4-1	Schematic of the Madistor Stepping Switch	23
4-2	Proposed Method of Operating Madistor as a Bandpass Filter	25
4-3	AC Equivalent Circuit of Madistor - Bandpass Filter	26
A-1	Commutated Filter Schematic	31
A-2	RC Charging Circuit	32
A-3	Time Quantized Sine Wave	34
A-4	Transfer Function Plot	38

LIST OF ILLUSTRATIONS (Cont'd.)

Figure		Page
B-1	Schmitt Trigger	40
B-2	Flip-Flop #1	40
B-3	"AND" Gate	41
B-4	Flip-Flop #2	41
B-5	Typical Isolation Amplifier with Switch	42
B-6	Overall Connection Procedure for All Bridges	42
B-7	Mixer Circuit Used to Measure Frequency Responses in the Vicinity of Resonant Peaks	43
B-8	Scope Photos of Various Circuit Waveforms	44
B-9	Scope Photos of Various Circuit Waveforms	45

1. Introduction.

A current trend in electronic circuitry is toward smaller and smaller components. New developments in micro-circuitry are being continually announced. Just about every type of circuit component can be packaged in a very small space. In fact, one of the real problems at present seems to be the attachment of external leads to these micro-circuits.

However, there is one important circuit component which, so far has escaped all attempts at micro-miniaturization, and that is the inductor. Without the inductor, circuits such as bandpass filters are exceedingly difficult to design.

The theory of commutated filters is well understood and a number of people have investigated commutated filter characteristics at audio frequencies^{/4/ /6/} and one team^{/2/} has reported on results at a center frequency of about 100 KC. RAPER^{/1/} has suggested the possibility of employing the commutated filter in the radio frequency range for IF filters etc.

The purpose of this paper is to report on investigations made with the RC sampled-data filter in the low and medium radio frequency range. Recommendations are made concerning the feasibility of this filter for r-f applications and the possibilities of adapting it for micro-miniature circuits.

The next section lays the basis for the theory of commutated filters and the mathematical derivation is completed in Appendix A. Following this, the design of a practical solid state filter is set forth. The circuit details appear in Appendix B.

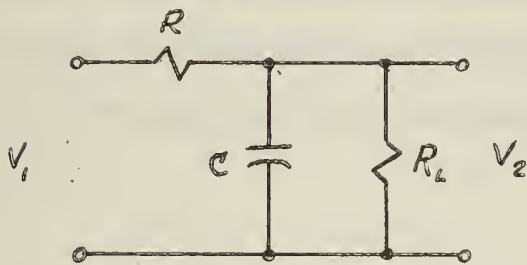
The fourth section describes a proposed circuit for a commutated filter employing a new solid state switching device, the MADISTOR⁵¹. Finally, recommendations and conclusions are made concerning the r-f applications of the sampled-data filter.

2. The Sampled-Data Bandpass Filter.

This section develops the theory of the sampled-data bandpass filter. The low pass filter is briefly discussed and this is logically evolved into the bandpass filter. The complete mathematical development, largely as set forth by LePage et al^{/3/} is contained in Appendix A.

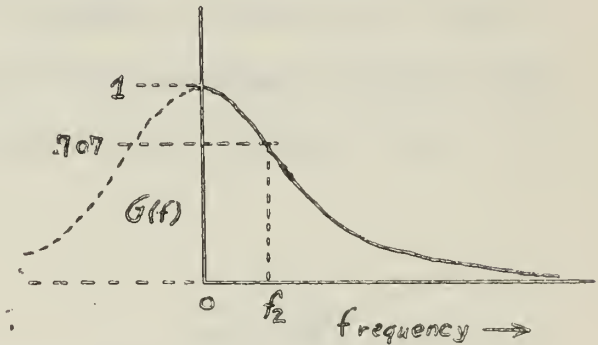
2-1 A Low Pass Filter.

The first step in the synthesis of the bandpass filter is to start with the well known RC low pass filter as in Fig. (2-1).



LOW PASS FILTER

Fig. (2-1)



FREQUENCY RESPONSE

Fig. (2-2)

The transfer function of this low pass filter $G(j\omega)$ is:

$$G(j\omega) = \frac{V_2}{V_1} = \frac{1}{1 + \frac{R}{R_L} j\omega RC}$$

$$\text{If } R_L \gg R; \quad G(j\omega) \cong \frac{1}{1 + j\omega RC}$$

Then $G(0) = 1$ and $G(\infty) = 0$. The curve is sketched in Fig. (2-2).

The bandpass limit of this low pass filter may be defined where:

$$|G(j\omega)| = \frac{G(j\omega)_{\max}}{\sqrt{2}}$$

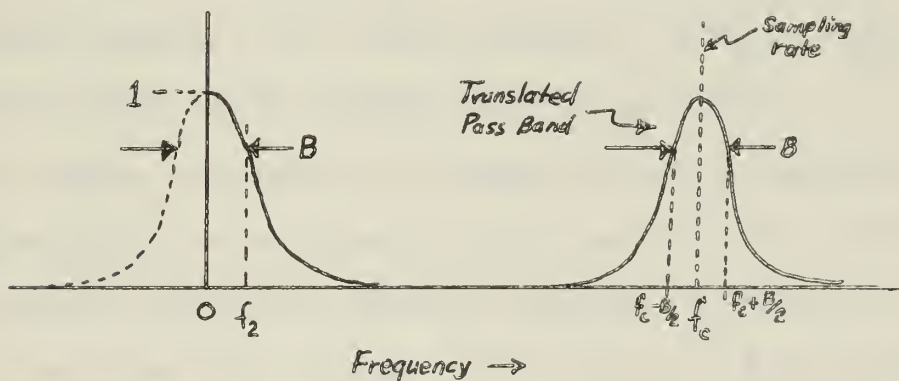
$$\text{Now, } G(j\omega) = \frac{1}{RC} \times \left[\frac{1}{\left(\frac{1}{RC} + j\omega \right)} \right] \quad \text{so, } \omega_2 = \frac{1}{RC} \quad \text{at the upper}$$

limit of the passband or $f_2 = \frac{1}{2\pi RC}$. The upper frequency limit or, as is common, the turn-over frequency, can be established at any value desired by appropriate selection of R and C.

2-2 Synthesis Of a Bandpass Filter.

It is not difficult to show that sampling an appropriate low pass RC filter at a certain sampling rate (f_c) results in translation in frequency of the filter response to a higher frequency. See Appendix A and /1/, /2/, /3/, /4/ and /6/.

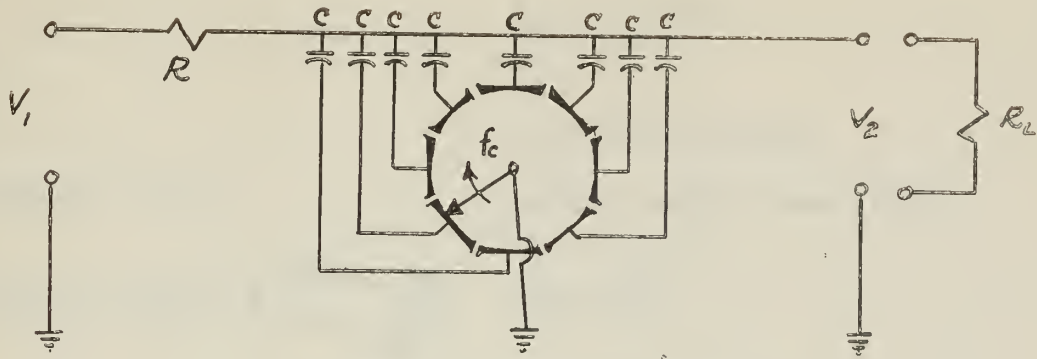
Another way of stating this is to consider the low pass filter as a bandpass filter whose center frequency is at zero c.p.s. This center frequency may then be translated to any higher frequency which is determined solely by the sampling rate (f_c) See Fig. (2-3).



TRANSLATION OF LOW PASS RESPONSE

Fig. (2-3)

This type filter is variously called a synchronous, sampled-data, or digital filter, and may be depicted schematically as a synchronous rotating commutator, as in Fig. (2-4).



SCHEMATIC OF SWITCHING COMMUTATOR

Fig. (2-4)

Thus, the commutator rotates at synchronous speed, grounding in turn each of the capacitors momentarily. If the commutator revolves at frequency f_c then the center frequency of the pass band is continuously variable from zero cycles per second up to the highest practicable speed of rotation of the mechanism.

One way of approaching the problem^{/4/} is to consider the unit impulse response of the series RC circuit. If $G(j\omega) = \frac{1}{RC} \frac{1}{(j\omega + \frac{1}{RC})}$ then the unit impulse response is $g(t) = \frac{1}{RC} e^{-t/RC}$. The rotating commutator can be thought of as a rectangular sampling pulse applied to the RC circuit every time the moving contact of the commutator touches each individual segment. If we assume each segment is very close to its neighbor and that there are N such segments equally distributed around the circumference, then one complete revolution of the moving "brush" would produce exactly N contiguous rectangular pulses. Each of these will be referred to as $s_1(t), s_2(t) \dots s_N(t)$.

So $S(t) = \sum_{n=1}^N s_n(t)$, where $S_1(t) = s(t)$
 $S_2(t) = s(t-2\tau)$

$$\begin{aligned}
 s_3(t) &= s(t-2\tau) \\
 &\vdots \\
 &\vdots \\
 s_N(t) &= s(t-(N-1)\tau)
 \end{aligned}$$

See Fig. (2-5).

Where τ = width of each pulse,

$$\text{and } s(t) = \frac{\tau}{T} \left[1 + 2 \sum_{n=1}^{\infty} \frac{\sin \frac{n\pi\tau}{T}}{\frac{n\pi\tau}{T}} \cos(\omega_n t) \right]$$

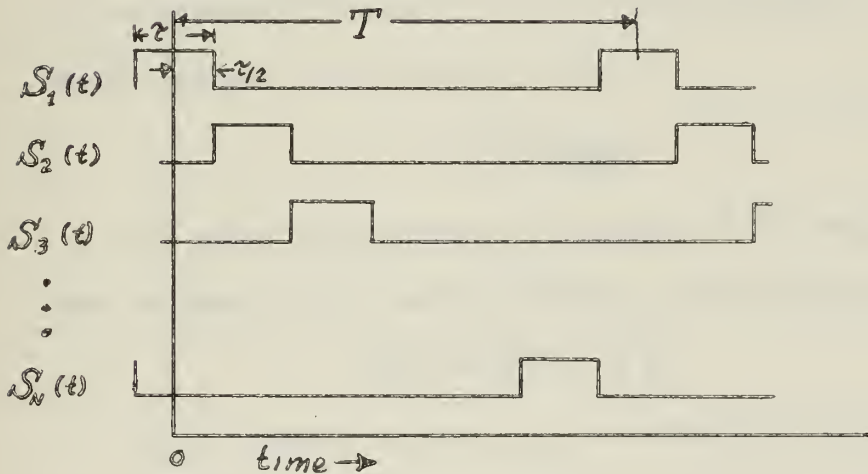
$$\omega_n = n\omega_1$$

$$\omega_1 = \frac{2\pi}{T}$$

T = period of rotation

τ , the pulse width, is the time required for the moving arm to traverse each segment.

$$\text{So } T = N\tau = \frac{1}{f_c} \text{ (no gaps between pulses)}$$



DEPICTION OF SAMPLING PULSES

Fig. (2-5)

The overall impulse response, $h(t)$ is:

$$h(t) = g(t)s(t)$$

$$= \frac{e^{-t/RC}}{2RC} \frac{\tau}{T} \sum_{m=1}^N \left[1 + 2 \sum_{n=1}^{\infty} \frac{\sin \frac{n\pi\tau}{T}}{\frac{n\pi\tau}{T}} \cos \omega_n \{t - \tau(m-1)\} \right]$$

From Appendix A, the transfer function $H(\omega T)$ is:

$$|H(\omega T)| = \frac{1}{\sqrt{1 + \left(\frac{2e^{-T/2RC} \sin(\frac{\omega T}{2})}{1 - e^{-T/RC}} \right)^2}}$$

Now in any conceivable practical r-f filter; $RC \gg T$. With this

assumption: $|H(\omega T)| \cong \frac{1}{\sqrt{1 + \left(\frac{2RC}{T} \sin(\frac{\omega T}{2}) \right)^2}}$

2-3 General Comments on Filter Characteristics.

The transfer function is accurately plotted as a function of frequency in Fig. (A-4) and is resketched as a function of f_c in Fig. (2-6). Note that theoretically the response of the filter is periodic with f_c and the magnitude of the response is 1 at all integer multiples of f_c .

The band width of each resonant peak is identical and independent of the resonant frequency. It is a function only of the number of capacitors and the product of R and C.

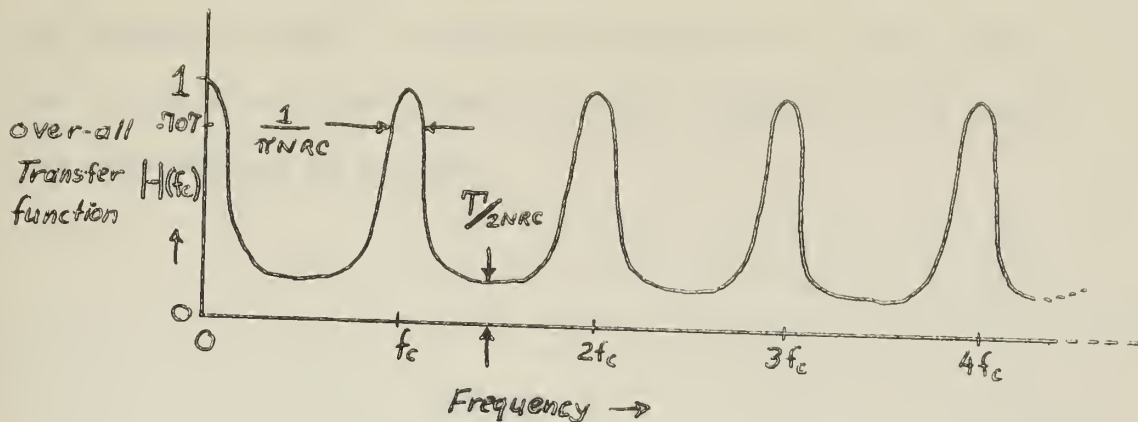
$$B \cong \frac{1}{\pi NRC}$$

The skirt selectivity is a function of the bandpass and the resonant frequency. The minimum response (in the rejection band) is:

$$|H_{\min}| \cong \frac{T}{2NRC} \cong \frac{\pi}{2} \frac{B}{f_c}$$

It is significant that H_{\min} is associated with the narrowest pass bands and contrary wise, a broad pass band results in very little rejection of unwanted frequencies between the resonant peaks.

In practice, the magnitude of higher harmonics of f_c may be appreciably reduced for reasons which will be discussed in a later section. If for any reason they should be troublesome, it would be no problem to attenuate them through a simple low pass filter across the output.



SKETCH OF TRANSFER FUNCTION $H(f_c)$

Fig. (2-6)

It is possible a higher harmonic of f_c might be desired. In such a case, a very broad band pass filter in series with the output would select the desired resonant response.

As an example of reasonable numbers which might be expected:

If $N = 8$

$$R = 100K \quad B = \frac{1}{8\pi \times 10^5 \times 10^{-9}} = \frac{10kc}{8\pi} \approx 400cps.$$

$C = 1000pf$

$$\text{Now if } f_c \approx 400kc, \quad Q_{\text{eff}} = \frac{400kc}{400cps} = 1000,$$

a fairly large value. In practice, Q could be made almost as large as desired.

While this device is shown as a rotating mechanical commutator, the sampling method will, of necessity, be by electronic means in order to obtain a filter useful in the r-f spectrum. One method which has been tried at audio frequencies^{/4/ /6/} and at low r-f frequencies^{/2/}, is to employ diode bridges as sampling devices to switch from one capacitor to another. Such a device was designed and built by the author, following a block diagram and the general procedures described

by FRANKS and WITT^{/2/}. This is the subject of the next section.
An alternate solid state sampling method (untested by the author)
is then proposed in section 4.

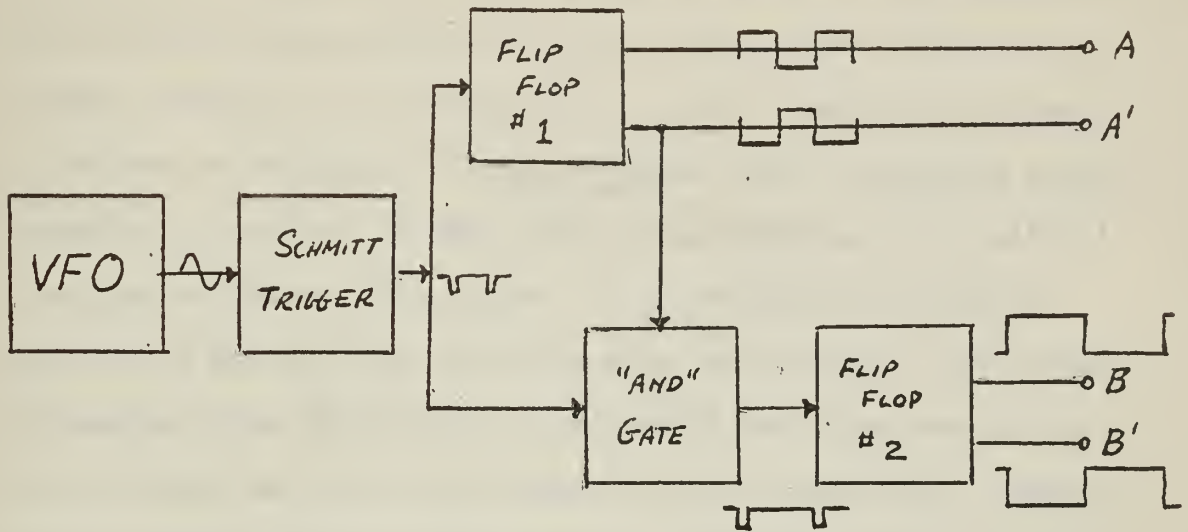
3. A Practical Solid State RC Filter.

3-1 Switch Considerations.

In order to make direct measurements of an operating RC filter in the radio frequency spectrum, a complete solid state commutating switch was built. For reasons which will become apparent later, certain parts of the switch could better be built with conventional electron tubes. However, transistors and semi-conductor diodes were utilized with the expectation that these circuits could eventually be miniaturized and integrated on to one common substrate. Thus, it might be possible to reduce an entire tunable band pass filter to a very small size. Such a circuit would have no inductors and no tuning capacitors. The assembly could be voltage tuned or synchronized to an external frequency source.

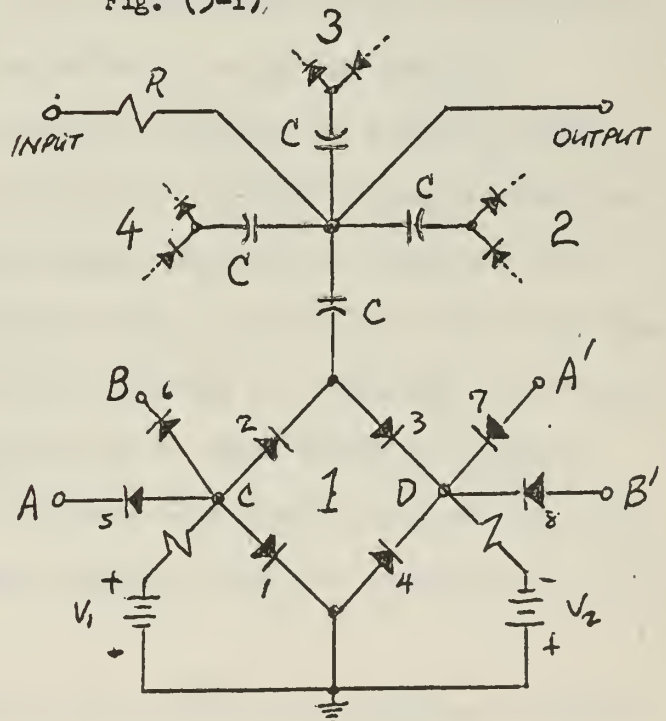
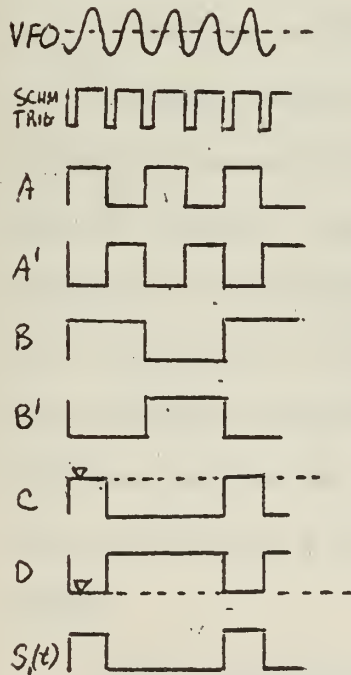
3-2 Operation of the Digital Switch.

Franks et al^{1/2/ 16/} have operated digital switches in the high audio and low r=f range. The set up of the author's switch follows a block diagram published by Franks^{1/2/}. Fig. (3-1) presents this arrangement and is taken directly from the referenced article. The circuit operates from any periodic waveform which will fire the schmitt trigger. The square wave output then drives two flip-flops, one of them through a gate so that only alternate pulses trigger the second flip-flop. Thus, the output waveforms are symmetrical square waves at one half and one quarter of the original input frequency. The relationship of these switching waves is shown in Fig. (3-2)^{1/2/}, also shown is how the wave forms combine in one of the four bridges to form a pseudo-rotating switch or sampling function.



BLOCK DIAGRAM FOR DIGITAL SWITCH^{2/}

Fig. (3-1).



RELATIONSHIP OF SWITCHING WAVEFORM ALONG WITH SCHEMATIC OF ONE OF FOUR IDENTICAL BRIDGES.

Fig. (3-2)

From inspection of Fig. (3-2), it is obvious the bridge forms a balanced diode modulator. With no inputs on any of the terminals, the two bias batteries, $+V_1$ and $-V_2$, will force current through the bridge, causing all four diodes (1, 2, 3, 4) to conduct and appear as a few ohms of resistance. Thus, the bridge can be replaced by a small resistor of less than 100 ohms, effectively grounding the capacitor connected at the top. When either of the switching waveforms is negative on the left side and positive on the right side, the series connecting diodes (5 or 6 and 7 or 8) act as "OR" gates and current flows through the gate diodes instead of the bridge diodes. Diodes (2 and 3) and (1 and 4) disconnect and the bridge "switch" is turned off. Examination of the waveforms in Fig. (3-2) reveals A or B are negative three out of the four periods of the cycle. Similarly, A^1 or B^1 are concurrently positive for the same three out of four intervals of the cycle. So, it is evident the batteries are permitted to turn "on" the switch one pulse out of every four periods.

By making connections as shown in Appendix B, different combinations of the waves A, B, A^1 and B^1 are applied to the terminals of the four bridges. Thus, each bridge conducts at a different time, in sequence. This sequence is shown in Fig. (3-3) which is also the same as in Fig. (2-5). So all of the conditions are satisfied for a commutating switch as described in section 2. This switch is slightly defective in that the "ON" resistance is a little less than 100 ohms, but this has only a very slight effect on the total operation of the device.

A more serious defect with this switch is the problem of synchronizing the four switching waveforms precisely so that the leading and trailing edges of the waves in Fig. (3-2) are exactly aligned.

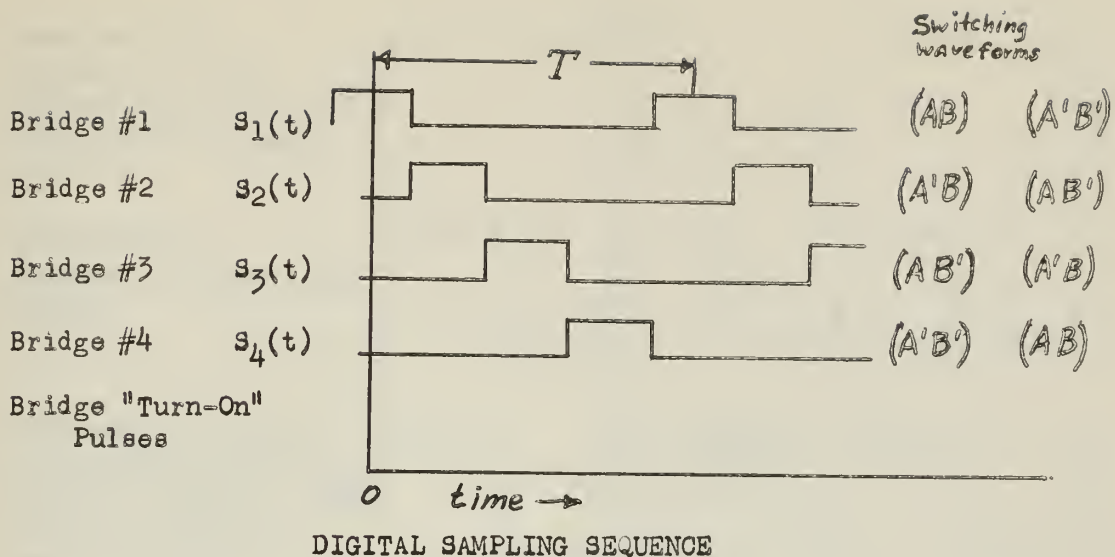


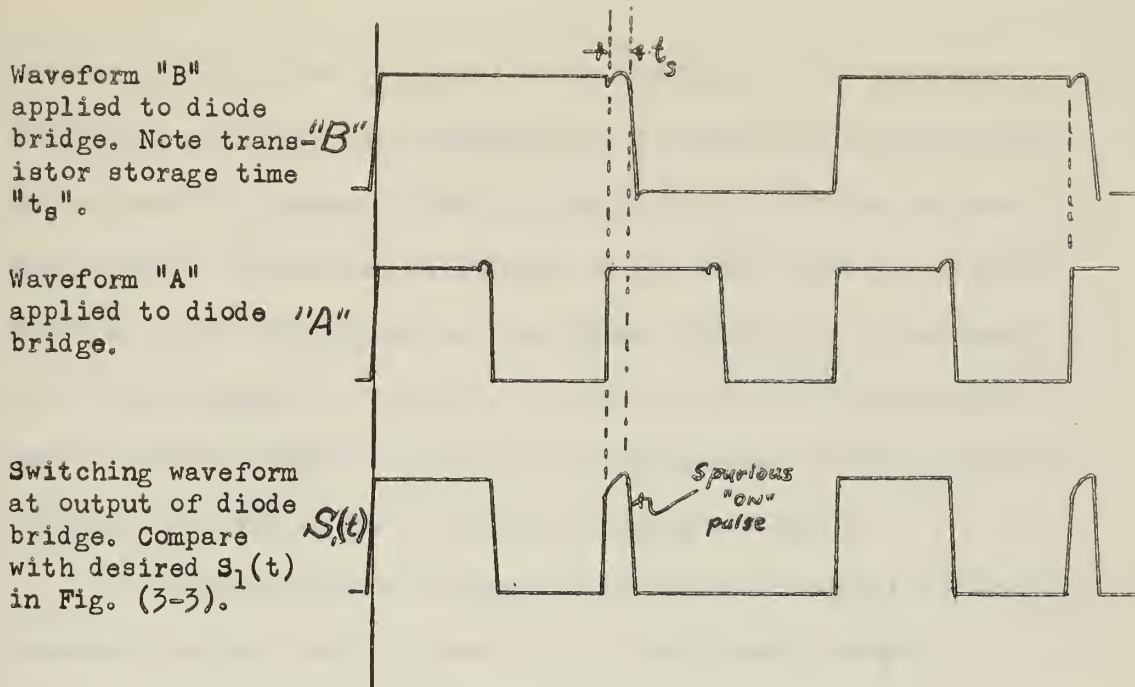
Fig. (3-3)

3-3 Discussion of Results Obtained from Operation of the Digital Switch.

The most serious operating problem with the filter is in supplying the driving power to the diode bridges. These bridges reflect a very heavy load back through the isolation amplifiers to the flip-flop circuits, gate and schmitt trigger. To supply power, the flip-flops were operated in a saturated condition. In addition to causing waveform distortions, the problem of transistor turn-off or storage time was encountered.

Fig. (3-4), taken from scope photos, shows how a spurious "ON" pulse appears in the output. This spurious "ON" pulse appears in the output as noise. Additionally, all of the various diodes contribute to the overall noise level in the output.

As can be seen from the output curves, probably the most serious defect of the digital switch at radio frequencies is the high noise level. The output noise represents approximately a constant 70-90 millivolts rms of voltage, almost entirely of a pulse nature, as can be seen from the pictures in Appendix B, Fig. (B-8) and (B-9).



SWITCHING SEQUENCE SHOWING DEFECTIVE SWITCHING ACTION
Fig. (3-4)

The only solution to the noise problem appears to be to provide more isolation between the flip-flops and the switch bridges. The flip-flops must operate at low level and be non-saturated in order to maintain precise pulse alignment.

The price for doing this is probably to double the number of transistors. At this point it becomes apparent that the ultimate goal of reducing the circuit size is being traded off in order to achieve reasonable noise figures.

Of course this type of noise problem is of very minor importance at audio or very low radio frequencies. Only as one increases f_c to the low and medium radio frequency band, does the noise problem get serious. The digital filter just described was operated at frequencies up to 250 KC with meter-measured transfer response out to 2 MC and observable oscilloscope response out to 10 MC.

Fig. (3-5) shows a typical filter response. For this plot, $R \approx 10K$, $C = .01 \mu f$. All harmonics of f_c (250 KC) were detectable out to the 40th harmonic (10MC) although above 2 MC the response was very slight. It was not measurable on the meter, but was readily detected on the oscilloscope. The theory predicts all responses to be of equal magnitude, however, as can be seen from the figure, in general each harmonic is diminished from the previous one. This anomaly is accounted for with the following reasoning:

1. The mathematical derivation is only approximate in that it assumes N large. In this case $N = 4$, a very small number.

2. RC was continually assumed to be much larger than the sample period. In this case $\frac{RC}{T} = 25$. The range of $\frac{RC}{T}$ for the circuits studied varied from a low of 2.5 to a high of 1250. In the case of the former, the circuit worked so poorly that the fundamental frequency ($f_c = 250$ KC) was barely detectable in the output. In the case of the latter, a very sharp response was observed. Values of RC employed were:

10, 20, 100, 200, 500, 1000 and 5000 micro-seconds.

In all cases except the one mentioned above, the response at 250 KCs was prominent and would be quite usable.

3. The bridge diodes are not ideal switches since they represent about 100Ω in series with the capacitor being switched, and ground. At frequencies greater than about 16 KC, the residual resistance of the bridge is equal to or greater than the reactance of a $0.1 \mu f$ capacitor.

Note in Fig. (3.5) that alternate harmonics of f_c are larger than the intermediate ones. ($f = .5, 1, 1.5, 2, 2.5 - -$ MCS). The reason for this is the following:

Due to the extremely narrow nature of all the pass bands, a small

amount of the signal frequency was coupled into the input of the switch oscillator, thus in effect synchronizing it with the signal. This procedure was necessary due to the poor stability of the oscillators and signal generators employed initially. The switch oscillator synched easier to .5, 1, 1.5 - - MCS than it did to .75, 1.25, 1.75 - MCS.

The signal rejection between resonant responses was not nearly as good as expected. A maximum of 20 db rejection was observed when the theoretical rejection should be 46 db (for $RC \approx .1ms$). Again, the defective switching waveform accounts for most of this. It was easily observable on the oscilloscope. The input signal was permitted to "leak" through the filter because of the spurious "on" pulse as shown in Figs. (3-4) and (B-9). This pulse permitted a constant amount (about 20 db) of input voltage to pass through the filter, thus limiting the maximum rejection attainable.

Notice that the high noise level at about -20 db also tended to mask low level signal measurements. This noise is a combination of spurious switching and diode noise. (see photographs in Fig. (9-B) p.45).

Due to the extremely narrow nature of the pass bands, a method had to be devised to measure deviations of as few as 2 or 3 cycles away from f_c . This was accomplished by synchronizing the switch filter to the P.G. School 100 KC high stability frequency standard and applying a signal generated from a General Radio 1330A bridge oscillator. These two frequencies were then mixed in a transistor chopper and the difference frequencies were separated and measured with a Hewlet Packard 500BR frequency meter. Using this method, the sides and peaks of a frequency response were examined in great detail. See Figs. (3-6), (3-7) and (3-8).

Fig. (3-6) shows a response for $RC \approx 100$ micro-seconds. (The same

time constant as in Fig. (3-5).)

Fig. (3-7) shows a response for $RC \approx 1000$ micro-seconds. The response is shown both expanded and compressed.

Fig. (3-8) shows the same ($RC \approx 1000$ micro-seconds) time constant. This figure is normalized with respect to $Q_0\delta$ as is commonly done.¹ In this case Q_0 was assumed to be $\frac{f_0}{B} = \frac{100 \text{ KC}}{540} = 185$. On the same graph is plotted a portion of a universal resonance curve from GRAY. It is noted the RC filter is very slightly narrower at the peak and has more rejection for values of $Q_0\delta > 1.0$, at least out to $Q_0\delta = 4.0$. The initial slope of the sides of the RC filter response are very nearly linear.

Another difference detected between theory and practice is the measured band widths. Again, this is accounted for by the approximately 20 db of spurious signal which was "leaking through" the filter. A comparison of observed and predicted band widths follows:

RC(μ sec.)	B(pred.)	B(obs.)
20	4 KC	18 KC
100	800	2 KC
1000	80	540
5000	16	Too narrow to measure

In summary, the greatest defects of the solid state commutated filter are the spurious signals and the high noise level.

The spurious signals are a result of the delayed switching signals from operating the flip-flops saturated. The noise comes from both this source and also the diode noise. The correction for the defect is to operate the flip-flops at very low level and provide maximum isolation

¹For instance, see: GRAY, Applied Electronics, 2nd Edition, John Wiley & Sons, 1954, page. 551.

between the load and the flip-flops. (Ideally, by a unilateral device such as a cathode follower.) Simple transistor circuits do not appear to be readily capable of providing the required isolation.

One very practical solution would be to use computer circuits and also computer cards for the circuits. This brings up another point. The circuits herein described were all bread-boarded on "Vector" type boards and there was doubtless considerable stray capacitance, series lead inductance and undesirable inter-circuit coupling of the signal at the radio frequencies employed.

Another partial solution of the problem would be to provide low noise type diodes for each of the 32 diodes in the four bridges.

FILTER RESPONSE
VERSUS
FREQUENCY

$f_c = 250 \text{ KC}$
 $R = 10 \text{ K}$ $RC = .1 \text{ ms}$
 $C = .01 \mu\text{f}$ $B = 800 \text{ cps}$

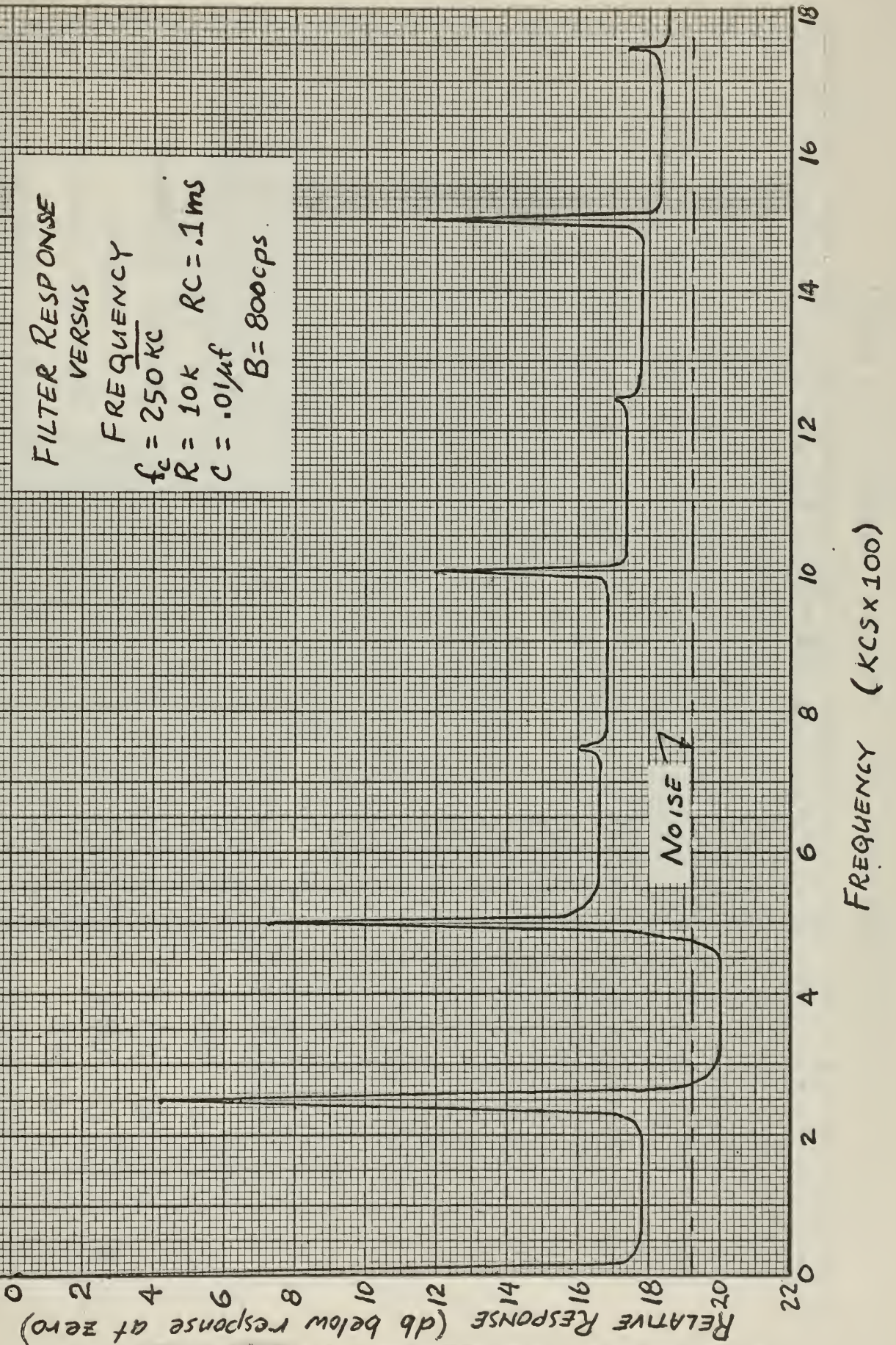


Figure (3-5)

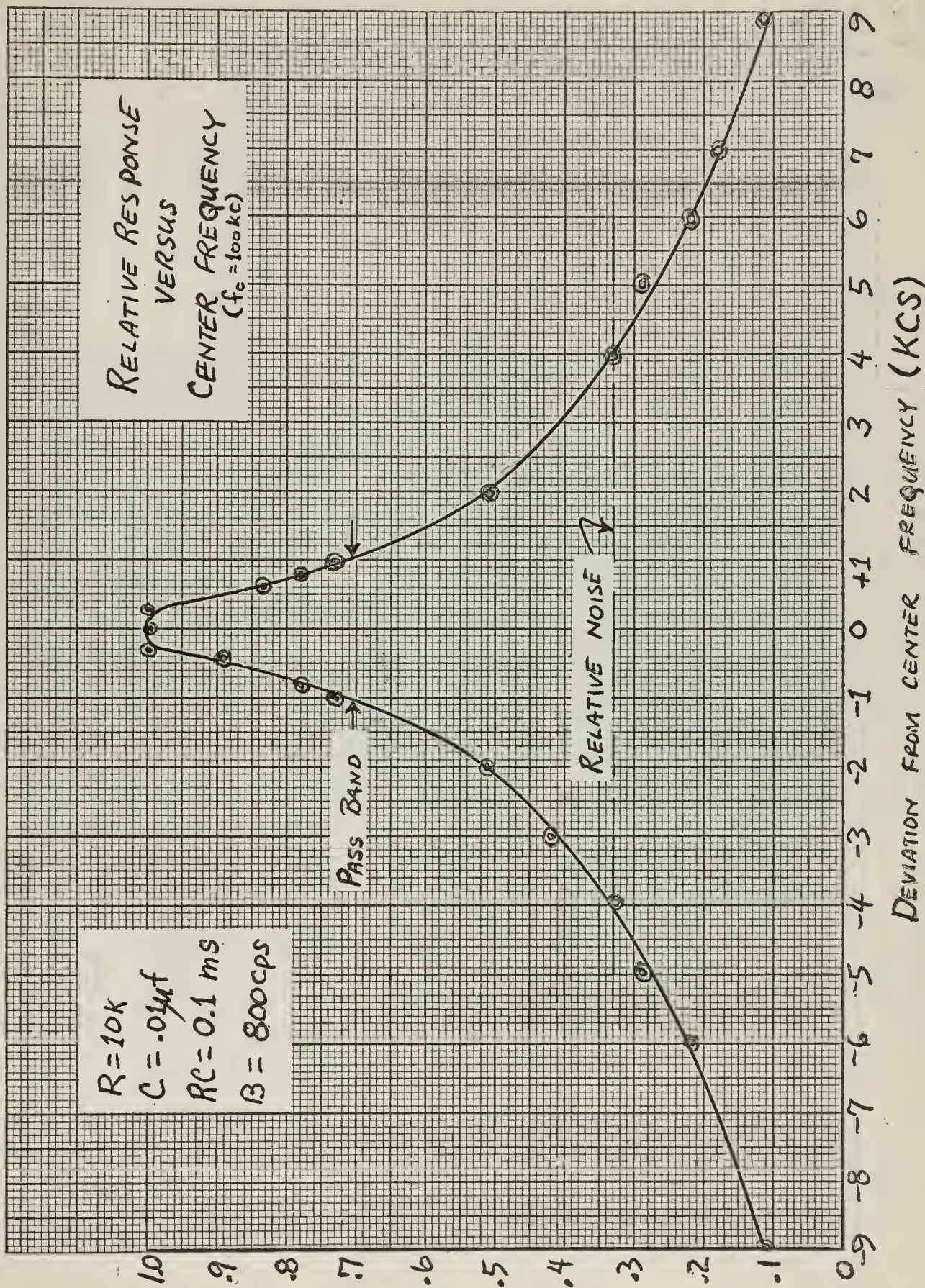


Figure (3-6)
20

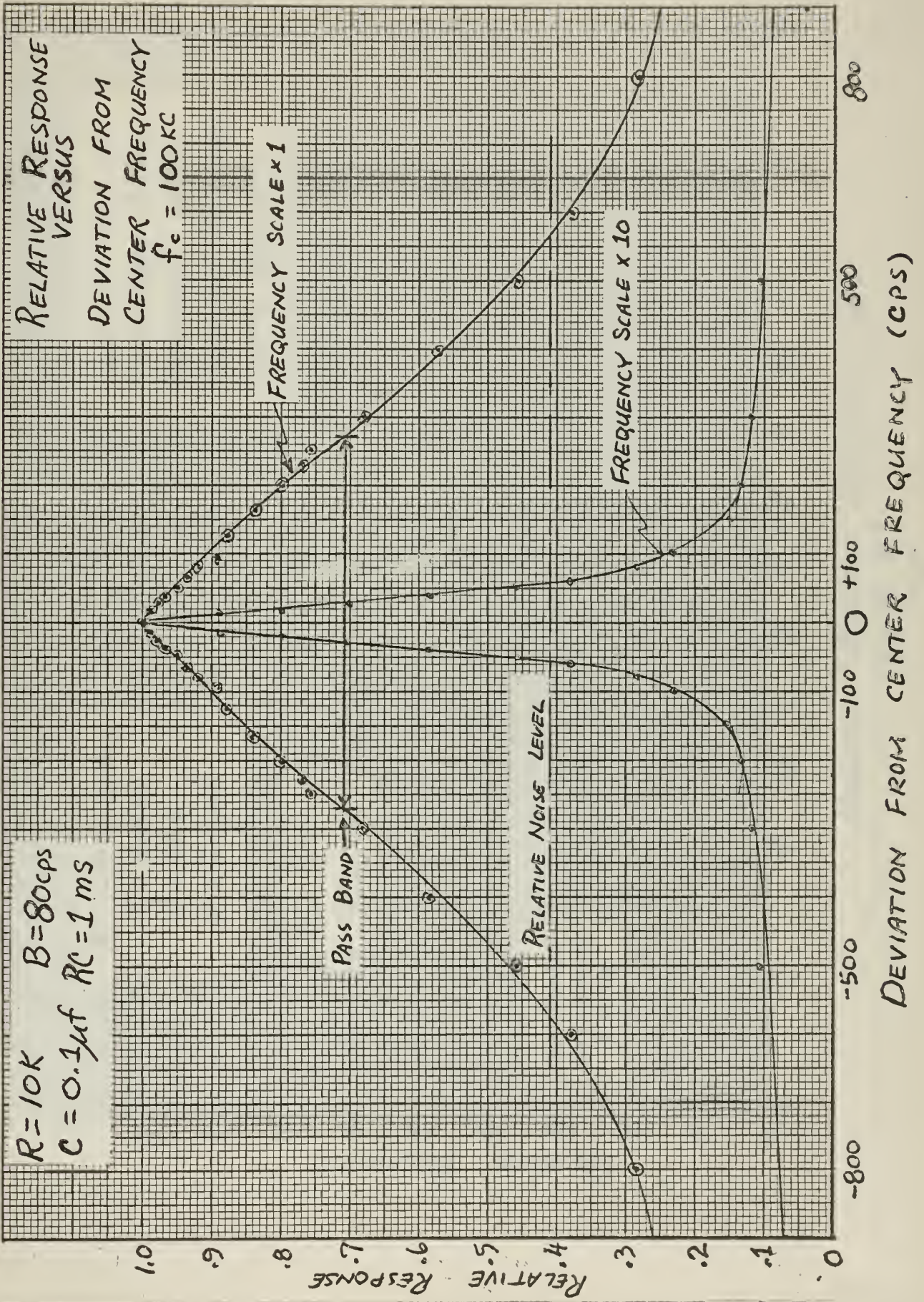


Figure (3-7)
21

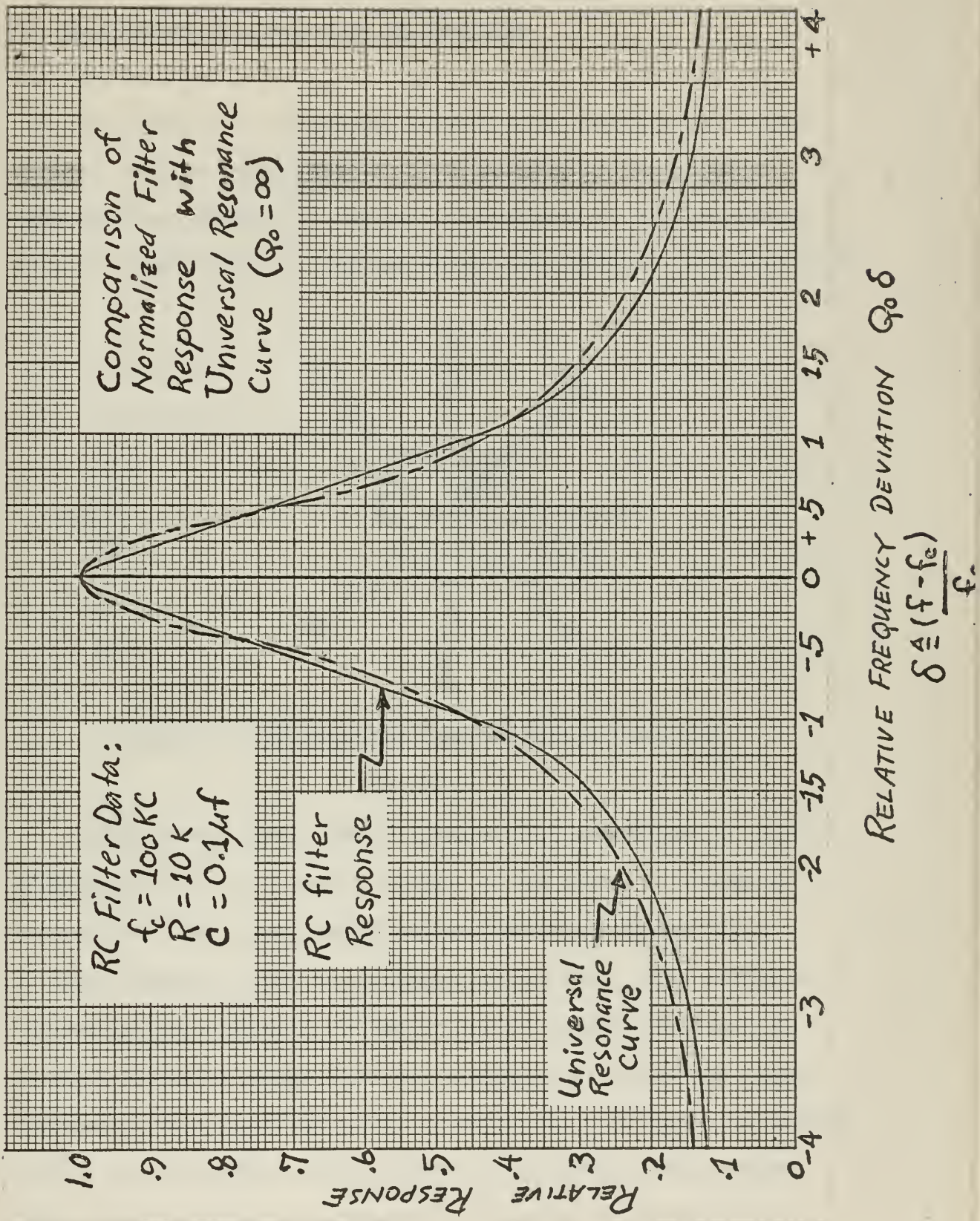
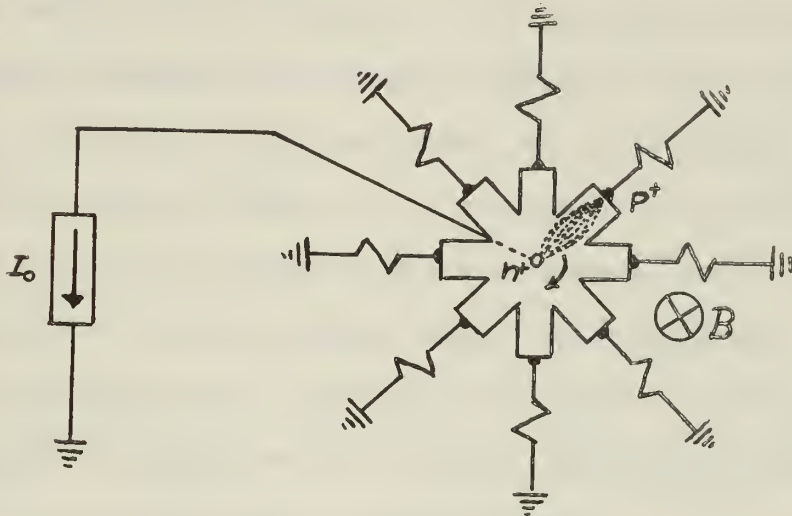


Figure (3-8)
22

4. An alternate Approach with the MADISTOR.

4-1 The Madistor.

The madistor is a magnetically controlled semiconductor plasma device. Various configurations of the madistor are described by MELNGAILIS and REDIKER^{/5/}, but the one pertinent to this discussion is the multiple based or stepping switch type madistor. See Fig. (4-1).



SCHEMATIC OF THE MADISTOR STEPPING SWITCH (FROM /5/)

Fig. (4-1)

Briefly, this device (which operates at a temperature of about 77°K) consists of an n^+ contact alloyed to the center of a disk of p-type InSb (Indium Antimonide) and any convenient number (N) of p^+ ohmic contacts around the periphery of the disk. When sufficient current is impressed upon the center contact (about 2 or 3 ma), an electron injection plasma forms and terminates at one of the output terminals. This injection plasma is stable and will remain indefinitely at some one output terminal unless it is moved by some external force. Such a force can conveniently be applied to the plasma by a perpendicular magnetic field of very moderate magnitude.

The plasma may be stepped in discrete steps from one terminal to another by a pulsing magnetic field perpendicular to the disk, or if a stronger steady state field is applied, the plasma will rotate continuously about the center contact. Minimum field strengths of the order of 0.5 gauss were required to switch the plasma from one output terminal to the adjacent one. (For comparison, the magnetic field of the Earth is about 0.6 gauss.) Field strengths stronger than the minimum switching field cause the plasma to rotate continuously, the rate of rotation being proportional to the magnitude of the magnetic field. Rotation speeds up to a maximum of about 17,000 revolutions per second were reported with a developmental model of the madistor having $N \approx 10$ ohmic contacts around the circumference. While 17 KC is definitely in the audio frequency range, it is felt this device is capable of development and consequent improvement of switching speed into the radio frequency operating range.

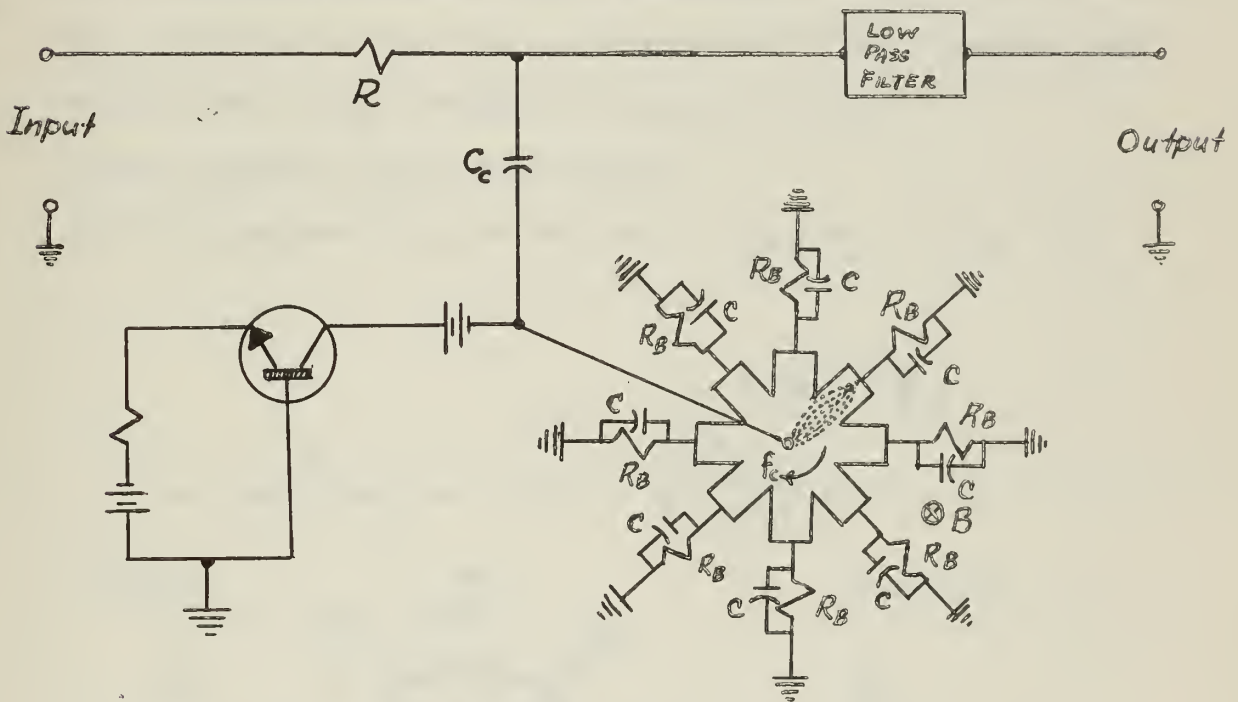
The entire madistor (including the coil required to produce the perpendicular magnetic field) is quite small and is capable of being entirely mounted on a TO-5 transistor header. (0.25 inches in diameter).

Presumably it would be possible to place consecutive circuits in tandem (stack them) so that one magnetic field would penetrate all of the InSb substrates simultaneously. Conceivably the electron plasmas in each of the madistors could be made to rotate synchronously, thus perhaps forming a series of identical band pass filters. This would have application as a radio receiver IF strip, or even as the front end of a tuned rf receiver.

4-2 Employing the Madistor as a Stepping Switch.

The madistor requires a certain minimum current to establish the injection plasma. Therefore, in operation, the device should be biased with a steady dc current supplied by a high impedance constant current source. Such a device might be a pentode vacuum tube or a transistor in the common base configuration.

One possible way of biasing the madistor, while at the same time superimposing the AC signal on it, might be as shown in Fig. (4-2).



PROPOSED METHOD OF OPERATING MADISTOR AS A BANDPASS FILTER

Fig. (4-2)

Each of the R_B 's is large compared with X_C of its parallel capacitor and is adjusted to limit the bias plasma current through the madistor to 2 or 3 ma. Also, C_c is large compared with C so that $X_{C_c} \ll X_C$ at the signal frequency. R is part of the RC required by the low pass filter which will determine the bandpass of the filter. ($B = \frac{1}{\pi NRC}$).

Note that the C referred to here is not the same C as in the original.

low pass case. Recall that $f_2 \approx B_{(\text{low pass})} = \frac{1}{2\pi RC}$

But $B_{(\text{commutated})} \approx NC_{(\text{commutated})}$, so $C_{(\text{low pass})} \approx NC_{(\text{commutated})}$

or $C_{(\text{commutated})} = \frac{C_{(\text{low pass})}}{N}$

From the example on page 8, $C_{(\text{commutated})} \approx 1000\text{pf}$, $N \approx 8$;

∴ $C_{(\text{low pass})} \approx NC_{(\text{commutated})} \approx 8 \times 1000 \text{ pf} \approx .008 \mu\text{f}$.

So $f_{2(\text{low pass})} \approx 200\text{cps}$.

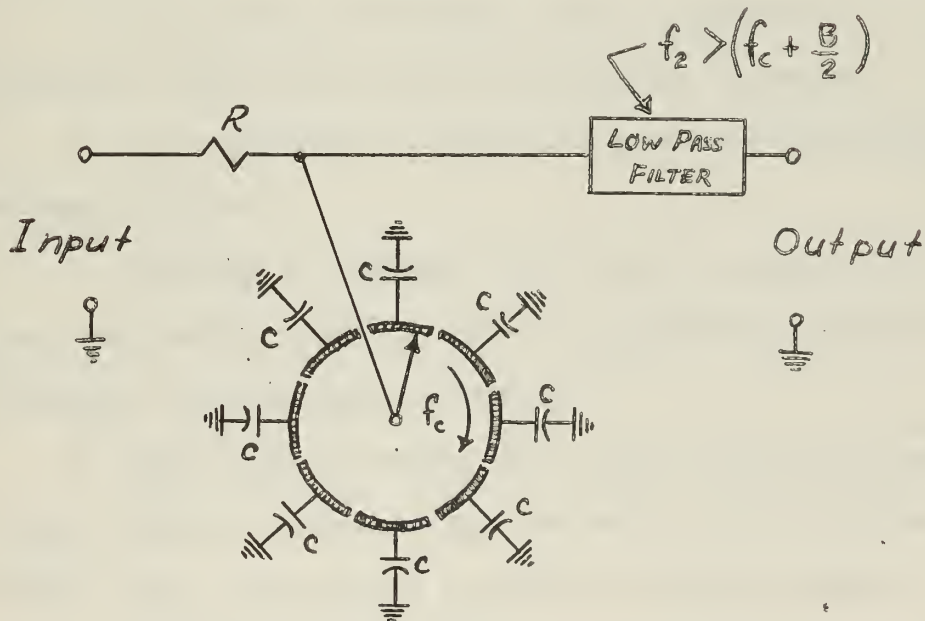
This corresponds to a pass band of 400 cps (200 cps either side of zero).

For a practical circuit, the output impedance of the transistor might

be about $1\text{M}\Omega$ and $R_B \approx 40\text{K} \gg X_c \approx 400\Omega$ at $f_c \approx 400 \text{ KC}$

$C_c \approx 0.1 \mu\text{f} \gg C \approx .001 \mu\text{f}$, thus $X_{C_c} \ll X_c$.

So the approximate AC equivalent circuit would be as in Fig. (4-3).



AC EQUIVALENT CIRCUIT OF MADISTOR - BANDPASS FILTER

Fig. (4-3)

Thus, we have an N-section electronic commutator. This then could be

the synchronous rotating device described earlier, in Section 2-2, and would complete the tunable bandpass filter.

4-3 Discussion and Summary of Madistor-Filter.

Although presently limited to a maximum switching frequency in the high audio frequency spectrum, it is felt the madistor offers considerable promise in the field of commutated filtering. It should be possible in the course of normal development to increase the upper frequency limit of the device by one and possibly by two orders of magnitude. If this could be accomplished, the broad field of radio frequency filters would be wide open for a really significant reduction in size of componentry.

Some features of the madistor operated RC filter are:

1. All parts of the circuit could be diffused on to a suitable substrate using rapid, accurate photographic techniques.
2. All components are compatible with current micro-miniaturization techniques.
3. Although an external coil of wire is required, it is very small and possibly could be used to simultaneously commutate several cascaded, identical bandpass filters.
4. The filter is tunable over a wide range with no movable parts. Only the current through the small coil of wire need be varied. Thus, the selected frequency is voltage tunable.
5. Very high Q filters with resultant narrow pass bands are attainable.

5. General Discussion, Conclusion and Recommendations.

Although there are a few difficult problems associated with the tunable RC bandpass filter, it has been demonstrated to be workable and useful in the radio frequency range. Situations in which this filter could be useful are:

1. Applications requiring a very narrow pass band at high frequencies (high effective Q).
2. Applications requiring a comb filter as in certain correlation filters.
3. Applications where an easily variable pass band is desired. (Replace the fixed R by a potentiometer.)
4. Applications where an inductor is not desired or can not be tolerated.
5. Applications requiring voltage tuning.
6. Potentially this circuit can be very greatly reduced in size, especially if the madistor filter described in Section 4 is utilized. (See summary of advantages of madistor filter at end of Section 4.)
7. It is conceivable this filter might be applicable in the field of intermediate frequency amplifiers.

The disadvantages, while few in number, are very serious:

1. Poor inter-band signal rejection (caused by spurious switching signal).
2. High diode noise level.
3. Complexity of balancing the diode balanced modulators for minimum noise.

4. In the case of transistor digital switching circuits, very poor isolation between the output and the switching elements, also inexact alignment of the switching pulses, causing spurious responses.

In general, the transistor switch appears to be somewhat limited in the r-f range, but very suitable in the audio to low r-f spectrum. The madistor seems to offer some hope in the future for development as a tunable bandpass filter.

There is still much work that can be done in this subject, particularly refinement of circuit details and packaging of components to reduce stray capacitance, series lead inductance and cross coupling between circuits.

It is hoped that this effort will be of assistance in further development of the RC bandpass filter.

BIBLIOGRAPHY

1. J.A.A. RAPER, Circuit Techniques and Microelectronics Systems. Electronic Products, September 1962.
2. L.E. FRANKS and F.J. WITT, Solid State Sampled-Data Bandpass Filters. Digest of Technical Papers, 1960 Solid State Circuits Conference, pp 70-71.
3. W.R. LePAGE, C.R. COHN and J.S. BROWN, Analysis of a Comb Filter Using Synchronously Commutated Capacitors. AIEE Trans. Part I, Vol. 72, 1953, pp 63-68.
4. B.D. SMITH, Analysis of Commutated Networks, IRE Trans. PGAE-10, pp 21-26.
5. I. MELNGAILIS and R.H. REDIKER, "The Madistor - a Magnetically Controlled Semiconductor Plasma Device". Proceedings of the IRE Vol. 50, pp 2428-35, December 1962.
6. L.E. FRANKS and I.W. SANDBERG, An Alternative Approach to the Realization of Network Transfer Functions: The N-Path Filter. Bell System Technical Journal, September 1960, pp 1321-50.
7. M. SCHWARTZ, Information Transmission, Modulation, and Noise. Chap. IV, McGraw-Hill Book Co., New York, 1959.
8. General Electric Transistor Manual, Sixth Edition, 1962.

APPENDIX A

COMMUTATED FILTER THEORY

The development in this Appendix, including most of the notation, largely follows that of LePAGE, COHN and BROWN^{13/}.

Definition of terms:

N = Number of capacitors.

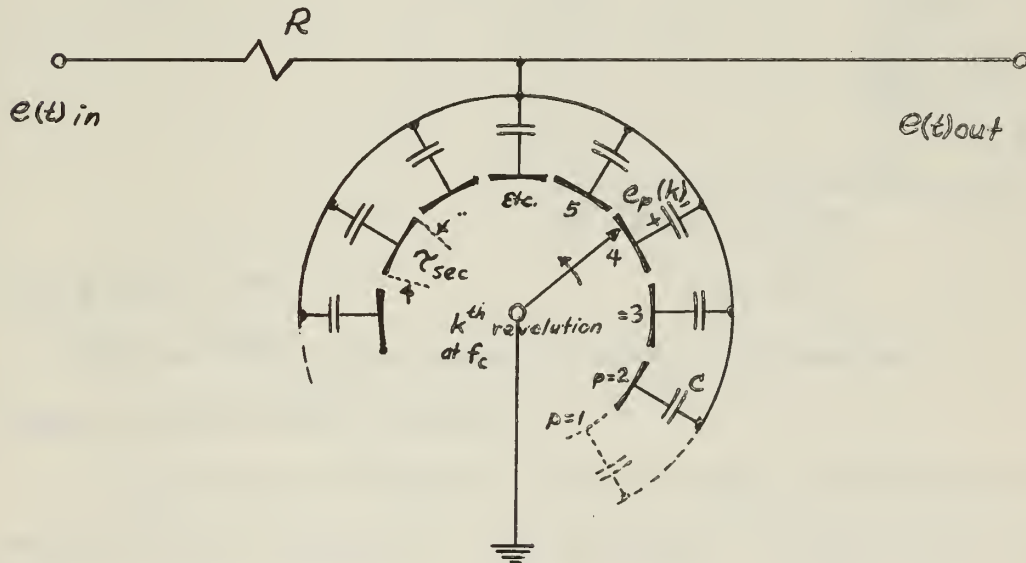
τ = Length of time brush is in contact with any one segment of the commutator.

T = Period of revolution of the brush around the commutator.
 $T = N\tau$ (segments are assumed to be contiguous).

f_c = Frequency of commutation. $f_c = \frac{1}{T}$

p = Identifying index for each segment around the periphery of the commutator.

k = Index for counting the number of revolutions from a reference time.



COMMUTATED FILTER SCHEMATIC

Fig. (A-1)

When the switch is placed in operation, all of the capacitors are assumed initially uncharged. At $t = 0$, rotation starts and, as each capacitor is grounded in turn, a small current flows on to the plates, depositing a small charge. As k becomes large, the charge on the

capacitors approaches a steady value and thus the voltage on each capacitor approaches a constant value. (This assumes the applied voltage is a steady sinusoidal function.)

Now the charge on each capacitor will change by only a very small amount during each revolution (assuming $RC \gg \tau$).

Let $e_p(k) \equiv$ voltage on capacitor (p) during revolution (k).

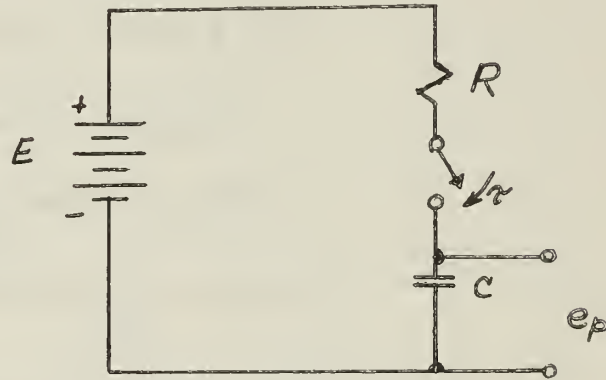
$\Delta e_p \equiv$ change in capacitor voltage during the time τ in any one revolution.

So, $e_p(\text{final}) \equiv e_p(\text{initial}) + \Delta e_p$ during the time τ .

$$e_p(\text{initial}) \triangleq e_p(k-1)$$

$$e_p(\text{final}) \triangleq e_p(k)$$

From Fig. (A-2):



RC CHARGING CIRCUIT

$$\Delta e_p \equiv E(1 - e^{-t/RC})$$

Fig. (A-2)

$$\equiv E(1 - e^{-\tau/RC}) \text{ if the switch is closed for } \tau \text{ seconds.}$$

$$\text{Where } E \equiv [e(p + kN)\tau - e_p(k-1)]$$

E represents the change in applied voltage from the end of the previous $(k-1)$ st revolution to the beginning of current (kth) revolution.

Substituting:

$$\begin{aligned} e_p(k) &\equiv e_p(k-1) + \Delta e_p \\ &\equiv e_p(k-1) + [e(p + kN)\tau - e_p(k-1)] (1 - e^{-\tau/RC}) \\ &\equiv e[(p + kN)\tau] (1 - e^{-\tau/RC}) + e_p(k-1)e^{-\tau/RC} \end{aligned}$$

Similarly, for previous revolutions of the brush,

$$e_p(k-1) = e^{-(p+(k-1)N)\tau} [1 - e^{-\tau/RC}] + e_p(k-2)e^{-\tau/RC}$$

$$\text{and } e_p(k-3) = e^{-(p+(k-2)N)\tau} [1 - e^{-\tau/RC}] + e_p(k-3)e^{-\tau/RC} \dots$$

$$\begin{aligned} \therefore e_p(k) &= e^{-(p+kN)\tau} [1 - e^{-\tau/RC}] + e^{-\tau/RC} \left\{ e^{-(p+(k-1)N)\tau} [1 - e^{-\tau/RC}] + e^{-\tau/RC} \times \right. \\ &\quad \left. \left\{ e^{-(p+(k-2)N)\tau} (1 - e^{-\tau/RC}) \dots \right\} \dots \right\} \\ &= \sum_{r=0}^k e^{-(p+(k-r)N)\tau} e^{-r\tau/RC} (1 - e^{-\tau/RC}) \\ &= (1 - e^{-\tau/RC}) \sum_{r=0}^k e^{-(p+(k-r)N)\tau} e^{-r\tau/RC} \end{aligned}$$

If the input is a sine wave; $e(t) = E \sin \omega t = E e^{j\omega t}$

$$e_p(k) = (1 - e^{-\tau/RC}) \sum_{r=0}^k E e^{j\omega[(p+(k-r)N)\tau]} e^{-r\tau/RC}$$

$$\text{Now } (p+(k-r)N)\tau = N\tau \left[\frac{p}{N} + (k-r) \right]; \text{ but } N\tau = \frac{1}{f_c}$$

$$= T \left[\frac{p}{N} + (k-r) \right]; \text{ let } \frac{p}{N} = \gamma$$

$$\begin{aligned} \text{Then } e_p(k) &= (1 - e^{-\tau/RC}) \sum_{r=0}^k E e^{j\omega T(\gamma+k-r)} e^{-r\tau/RC} \\ &= (1 - e^{-\tau/RC}) E e^{j\omega T(\gamma+k)} \sum_{r=0}^k e^{-r(j\omega T + \tau/RC)} \\ &= E(1 - e^{-\tau/RC}) e^{j\omega T(\gamma+k)} \sum_{r=0}^k e^{-(\tau/RC + j\omega T)r} \end{aligned}$$

$$\text{But } \sum_{r=0}^k e^{-ar} = \frac{1 - e^{-a(k+1)}}{1 - e^{-a}} \quad \text{for } k \text{ terms of a geometric series.}$$

$$\text{So } e_p(k) = \frac{E(1 - e^{-\tau/RC}) e^{j\omega T(\gamma+k)} (1 - e^{-(\tau/RC + j\omega T)(k+1)})}{1 - e^{-(\tau/RC + j\omega T)}}, \text{ this}$$

is the voltage on any capacitor (p) after the k^{th} revolution.

[The text on this page is extremely faint and illegible. It appears to be a list or a series of entries, possibly names and dates, but the characters are too light to transcribe accurately.]

Now in a practical filter $RC \gg T$, by a factor of one to two orders of magnitude, but as k gets very large; $\left[(k+1) \frac{T}{RC} \right]$ grows large. As this term grows very large, $e^{-(T/RC + j\omega T)(k+1)}$ approaches zero, since the term $|e^{-j\omega T(k+1)}| = 1$.

$$\text{So, } e_p(k) = \frac{E(1 - e^{-T/RC})e^{j\omega T(\gamma+k)}}{1 - e^{-(T/RC + j\omega T)}} = \frac{E(1 - e^{-T/RC})\sin[\omega T(\gamma+k)]}{1 - e^{-(T/RC + j\omega T)}}$$

If $E_0 \triangleq \frac{E(1 - e^{-T/RC})}{1 - e^{-(T/RC + j\omega T)}}$, then:

$$e_p(k) = E_0 \sin \omega T(\gamma+k) = E_0 \sin \omega T(p+Nk)$$

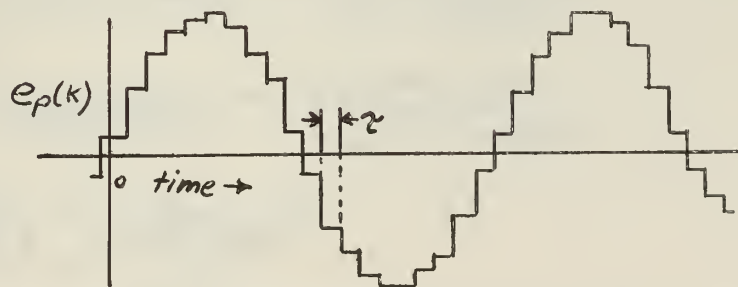
Now $(p+Nk)$ represents a discrete time function which advances in increments of T , the time between centers of the commutator segments.

For example, if $N = 4$; $(p+Nk) = (p+4k)$ starts at an initial position and advances one unit at a time, i.e., $(p+4k) = 1, 2, 3, 4, (1+4), (2+4), (3+4), (4+4), (1+8), \text{ etc.}$ That is, p ranges from 1 to 4 and

then k advances by one and p again ranges from 1 to 4 etc. As far

as the output is concerned, the function can be replaced by: $\sum_{i=1}^{\infty} \omega T(j)$.

So $e_p(k) = E_0 \sin\left(\sum_{i=1}^{\infty} \omega T i\right)$; thus a sine wave input will come out as a quantized sine wave.



TIME QUANTIZED SINE WAVE

Fig. (A-3)

If the steps are small enough this will be a very close approximation to the input sine wave. Alternately, passing the output wave through a low pass filter will essentially restore the original sine wave shape.

Therefore, the argument $(\sum_{i=1}^{\infty} \omega \tau_i)$ approaches (ωt) .
 So $e_o(t) \cong E_o \sin(\omega t)$, which is the same as the input with E replaced by E_o .

$$\frac{e_o(t)}{e_{in}(t)} = \frac{E_o \sin(\omega t)}{E \sin(\omega t)} = \frac{E_o}{E} = \frac{E(1 - e^{-\tau/Rc})}{e(1 - e^{-(\tau/Rc + j\omega T)})}$$

the transfer function $H(\omega T) = \frac{e_o(t)}{e_{in}(t)} = \frac{1 - e^{-\tau/Rc}}{1 - e^{-(\tau/Rc + j\omega T)}}$

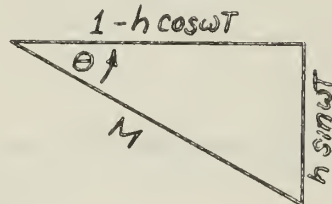
How $H(\omega T)$ is a periodic function of frequency and is equal to:

$$H(\omega T) = \frac{H}{\theta}$$

where $H = |H(\omega T)|$ & $\theta = \angle H(\omega T)$ let $e^{-\tau/Rc} \triangleq h$

$$H = \frac{1-h}{1 - h e^{-j\omega T}} = \frac{1-h}{1-h[\cos(\omega T) - j \sin(\omega T)]}$$

$$\begin{aligned} M &= \sqrt{(1-h \cos \omega T)^2 + h^2 \sin^2 \omega T} \\ &= \sqrt{1 - 2h \cos(\omega T) + h^2 \cos^2(\omega T) + h^2 \sin^2(\omega T)} \\ &= \sqrt{1 - 2h \cos(\omega T) + h^2} = \sqrt{(1+h^2 - 2h) + 2h - h \cos(\omega T)} \\ &= \sqrt{(1-h)^2 + 2h(1 - \cos \omega T)} = (1-h) \sqrt{1 + \frac{2h(1 - \cos \omega T)}{(1-h)^2}} \end{aligned}$$



$$\theta = \tan^{-1} \left(\frac{h \sin(\omega T)}{1-h \cos(\omega T)} \right) = \tan^{-1} \left(\frac{e^{-\tau/Rc} \sin(\omega T)}{1 - e^{-\tau/Rc} \cos(\omega T)} \right)$$

$$\text{So } H = \frac{1-h}{M/\theta} = \frac{\theta}{\sqrt{1 + \frac{2h(1 - \cos \omega T)}{(1-h)^2}}}$$

The most interesting characteristic of this transfer function is the periodicity of the magnitude of H .

$$|H(\omega T)| = \frac{1}{\sqrt{1 + \left(\frac{2e^{-\tau/RC} \sin(\frac{\omega T}{2})}{1 - e^{-\tau/RC}} \right)^2}} \quad ; \quad \text{this function is plotted in Fig. (A-4).}$$

Maximum response:

$$\text{Now } 1 - e^{-\tau/RC} = 1 - 1 + \frac{\tau}{RC} - \frac{\tau^2}{2(RC)^2} + \dots \approx \frac{\tau}{RC}$$

$$\text{and } e^{-\tau/2RC} \approx 1 \quad \text{if } RC \gg \tau$$

So

$$|H(\omega T)| \approx \frac{1}{\sqrt{1 + \left(\frac{2RC}{\tau} \sin(\frac{\omega T}{2}) \right)^2}} = \frac{\tau}{2RC} \frac{1}{\sqrt{\left(\frac{\tau}{2RC} \right)^2 + \sin^2(\frac{\omega T}{2})}}$$

When $\omega T = 0, 2\pi, 4\pi, \dots, 2n\pi$; $\sin(\omega T) = 0$

$$\therefore |H(2n\pi)| = \frac{\tau}{2RC} \frac{1}{\sqrt{\left(\frac{\tau}{2RC} \right)^2}} = 1 \quad (\text{a maximum response})$$

Minimum response:

Similarly, when $\omega T = \pi, 3\pi, 5\pi, \dots, (2n+1)\pi$; $\sin(\frac{\omega T}{2}) = 1$

$$\text{Since } \frac{\tau}{RC} \gg 1, \quad |H[(2n+1)\pi]| \approx \frac{\tau}{2RC} = \frac{T}{2NRC}$$

So the magnitude of the minimum response $\approx \frac{T}{2NRC}$, the maximum is 1

and the peaks are seen to be periodic and occur when

$$\omega T = 2\pi n \quad \text{or} \quad 2\pi f/f_c = 2\pi n \quad \text{So } f/f_c = n \quad (n = \text{integer})$$

whenever f is equal to any integer multiple of f_c .

Band width:

The band width of the output occurs when the magnitude of the output voltage drops to $\frac{1}{\sqrt{2}}$ peak value.

$$\text{or } |H(\omega T)| = \frac{1}{\sqrt{2}} = \frac{1}{\sqrt{1 + \left(\frac{2RC}{\tau} \sin \frac{\omega T}{2} \right)^2}} \quad \text{or } \frac{2RC}{\tau} \sin \frac{\omega T}{2} = 1$$

so $\sin\left(\frac{\omega T}{2}\right) = \frac{\tau}{2RC}$ since $\frac{\tau}{2RC} \ll 1$

one can approximate $\sin\frac{\omega T}{2}$ by the first term of the power series:

$$\sin \frac{\omega T}{2} = \frac{\omega T}{2} - \frac{\left(\frac{\omega T}{2}\right)^3}{3!} + \dots \approx \frac{\omega T}{2} \quad \text{So, } \omega T = \frac{2\tau}{RC}$$

This is the first 3 db point. The second will occur at $2\pi - \frac{2\tau}{RC}$, the

third at $2\pi + \frac{2\tau}{RC}$. In general, the half power points occur when:

$$(\omega T)_{3db} = 2n\pi \pm \frac{2\tau}{RC}$$

the bandwidth then is: $(2n\pi + \frac{2\tau}{RC}) - (2n\pi - \frac{2\tau}{RC}) = \frac{2\tau}{RC}$

$$2\pi f T = \frac{2\tau}{RC} = \frac{2T}{NRC}$$

so $B = \frac{1}{\pi NRC}$

where B = bandwidth (cps),

PLOT OF TRANSFER FUNCTION $|H(f)|$ FOR
 RC FILTER VERSUS FREQUENCY
 where $|H(f)| = [1 + (\frac{2RC}{T} \sin \pi f T)^2]^{-1/2}$

$B = 8 \text{ KC}$
 $N = 4$
 $RC = 10 \mu\text{s}$

$f_c = 100 \text{ KC}$
 $R = 1 \text{ K}\Omega$
 $C = 0.01 \mu\text{f}$

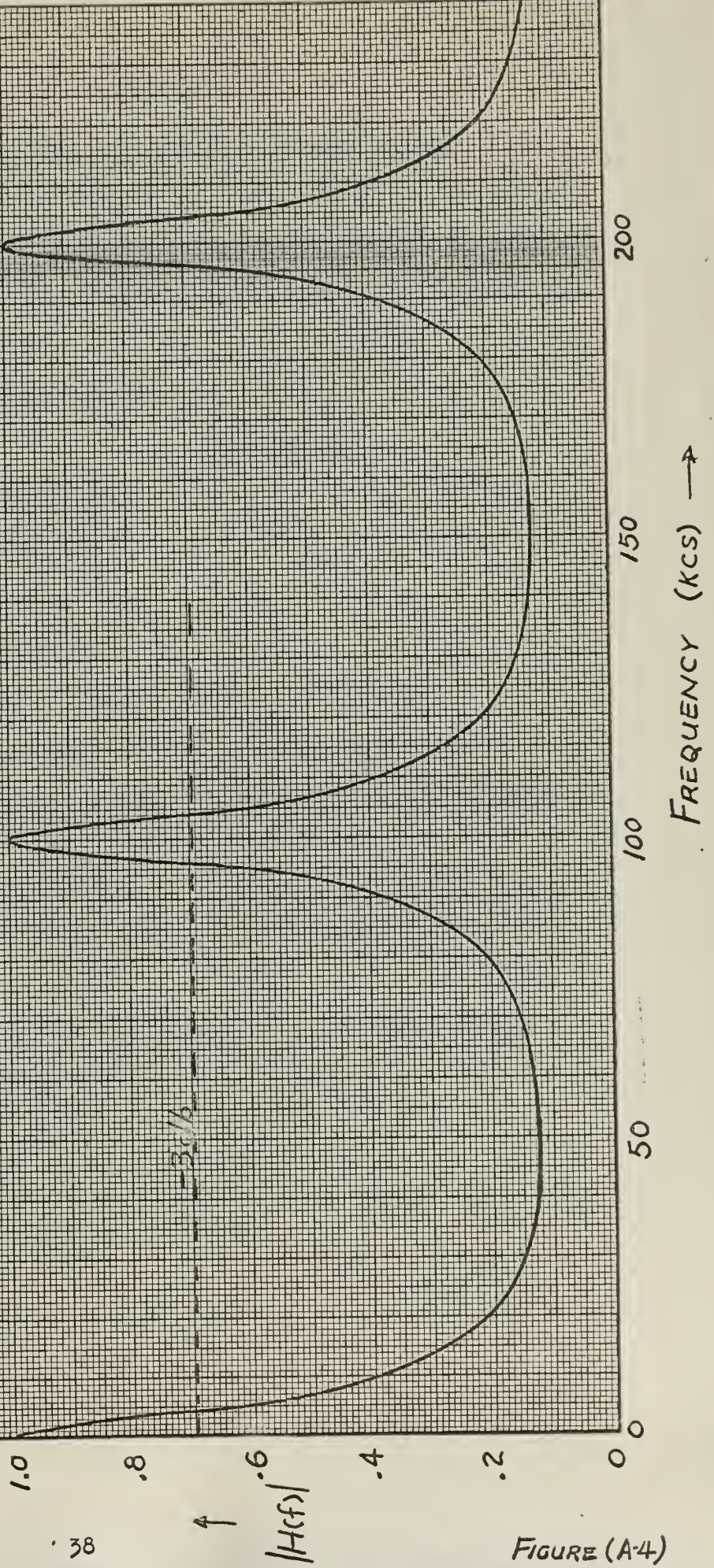


FIGURE (A-4)

APPENDIX B

Circuit Details of a Practical Bandpass Filter

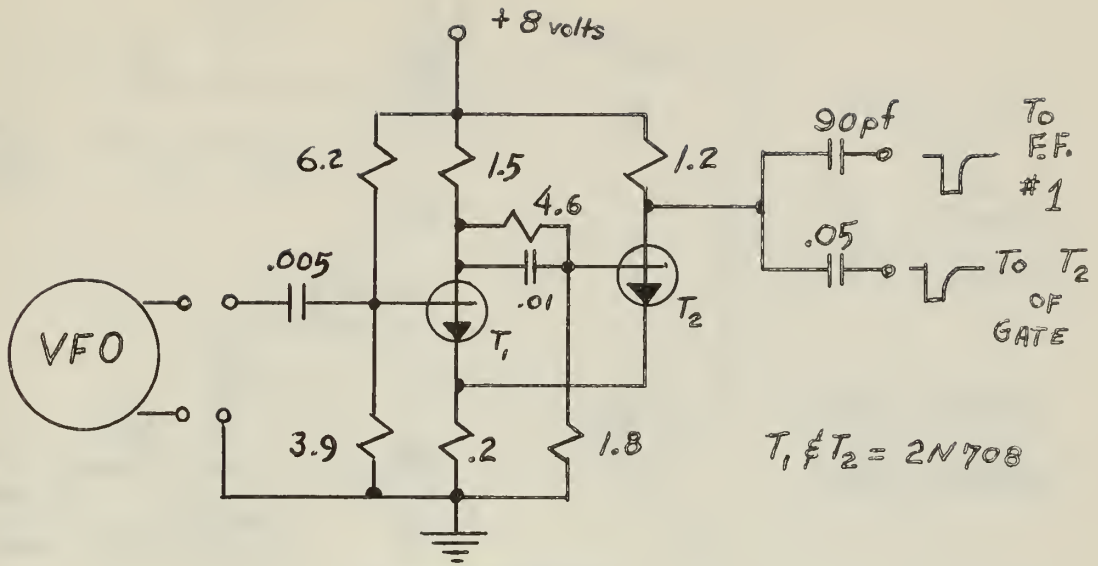
The following circuit diagrams give the details of the circuits which were employed to obtain the data presented in Section III. The circuits are grouped into the appropriate blocks as outlined on page 11, Figs. (3-1) and (3-2).

A summary of diagrams follows:

<u>Figure</u>	<u>Description</u>
B-1	Schmitt Trigger
B-2	Flip-Flop #1
B-3	"AND" Gate
B-4	Flip-Flop #2
B-5	Typical Isolation Amplifier with Switch
B-6	Overall Connection Procedure for all Bridges
B-7	Mixer Circuit used to Measure Frequency Responses in the Vicinity of Resonant Peaks
B-8 & B-9	Scope Photos of Various circuit Waveforms

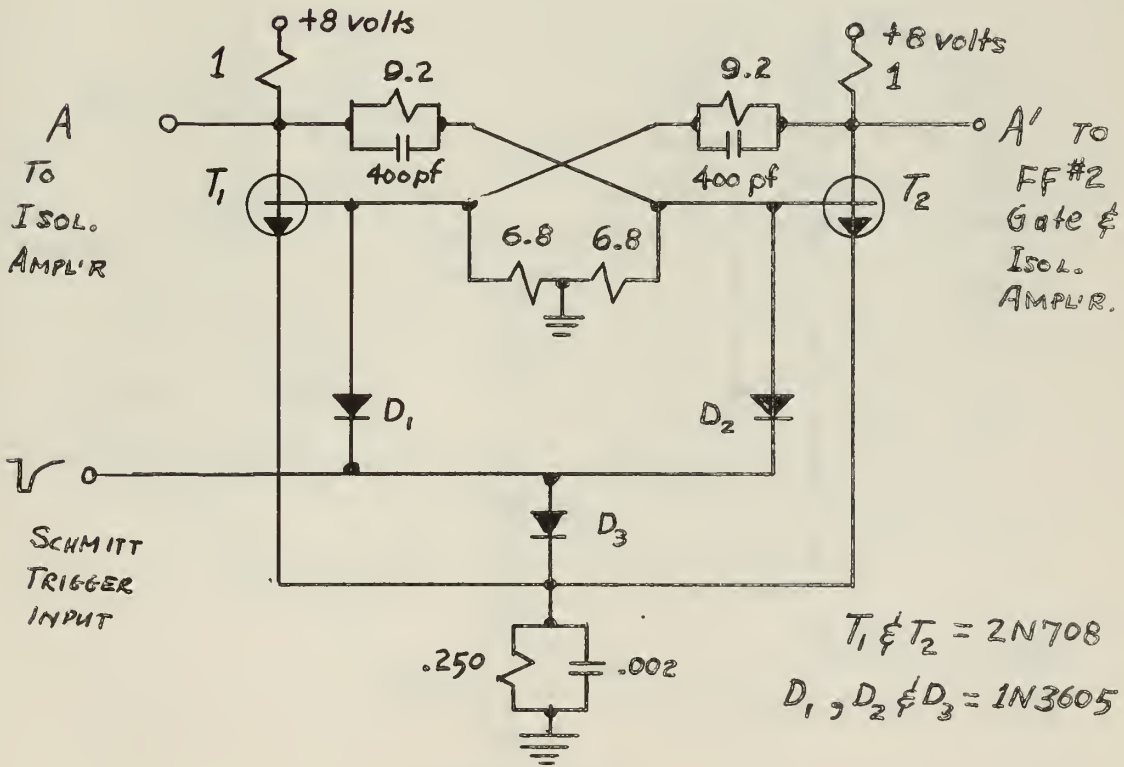
Unless otherwise stated, all resistors are K ohms and all capacitors are μf .

Most of the circuit calculations are based on data obtained from the GE Transistor Manual. /8/



SCHMITT TRIGGER

Fig. (B-1)



FLIP-FLOP #1

Fig. (B-2)

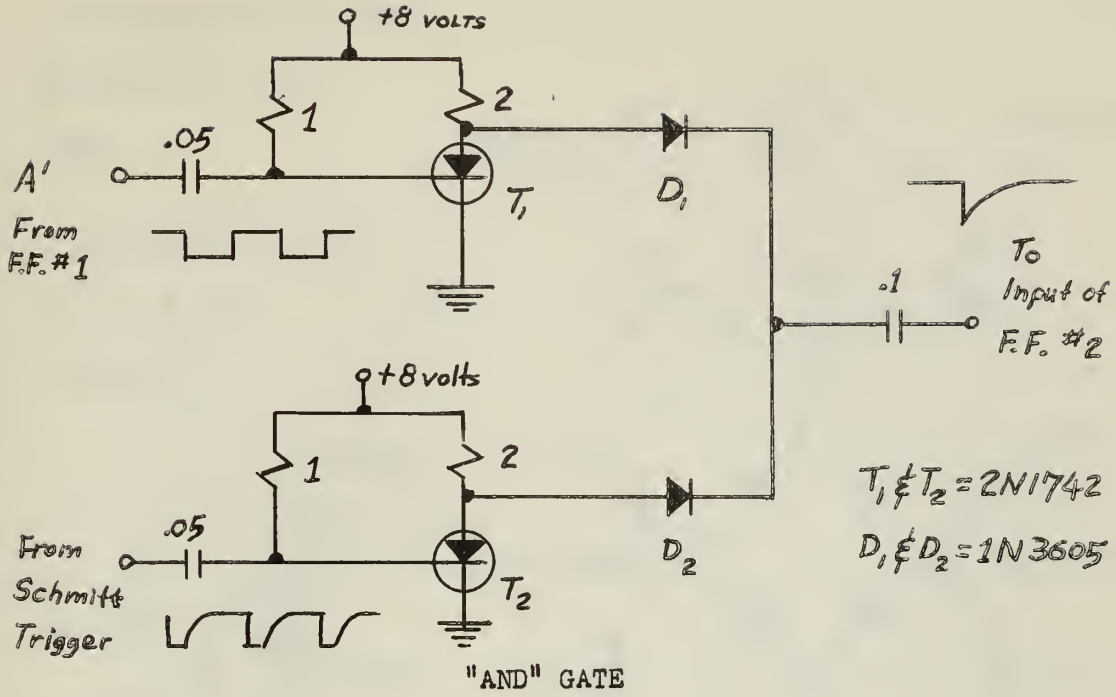


Fig. (B-3)

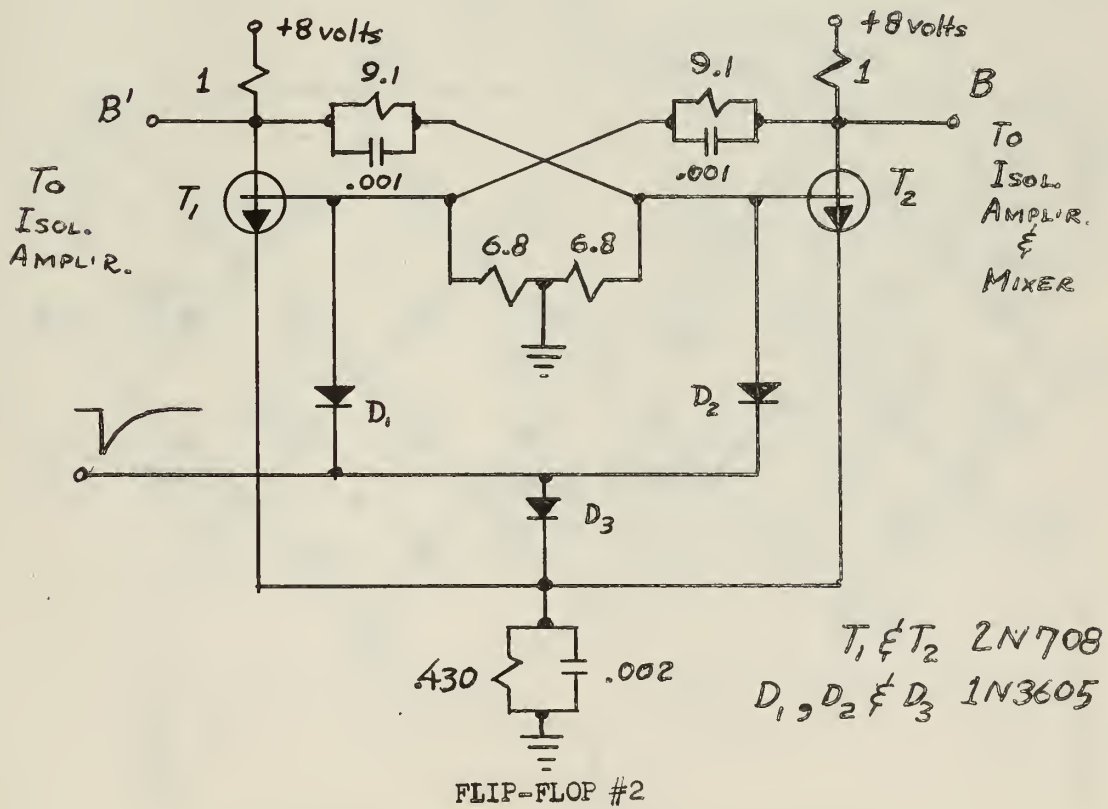
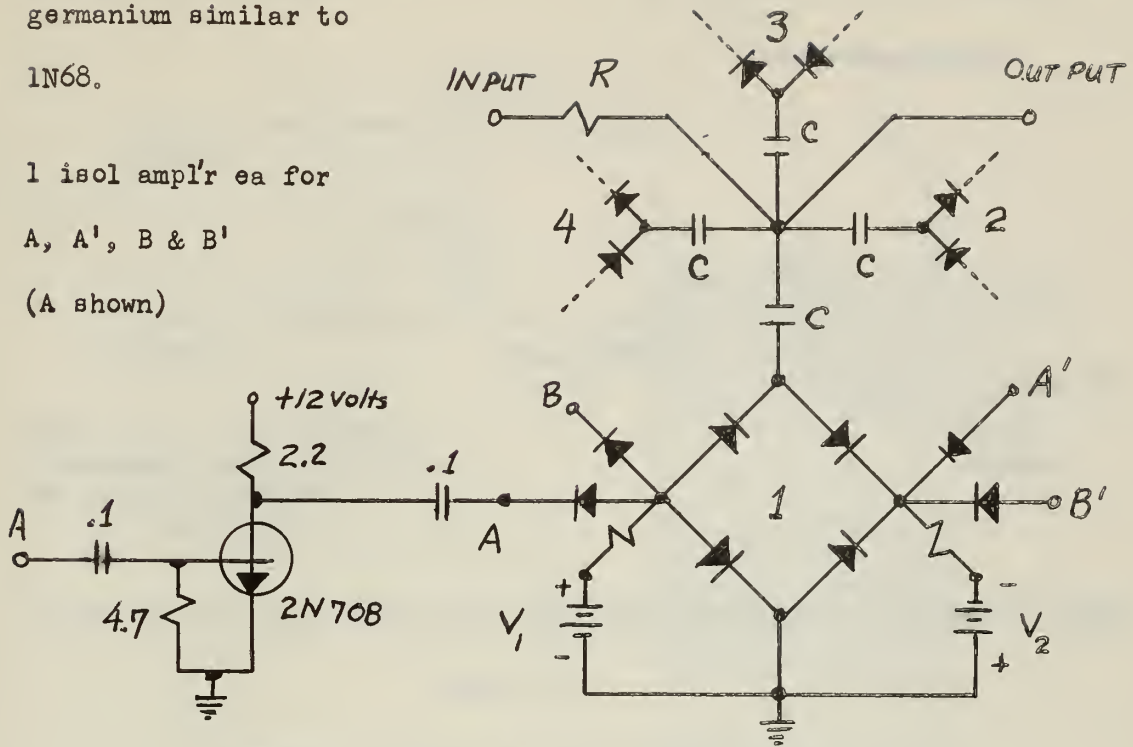


Fig. (B-4)

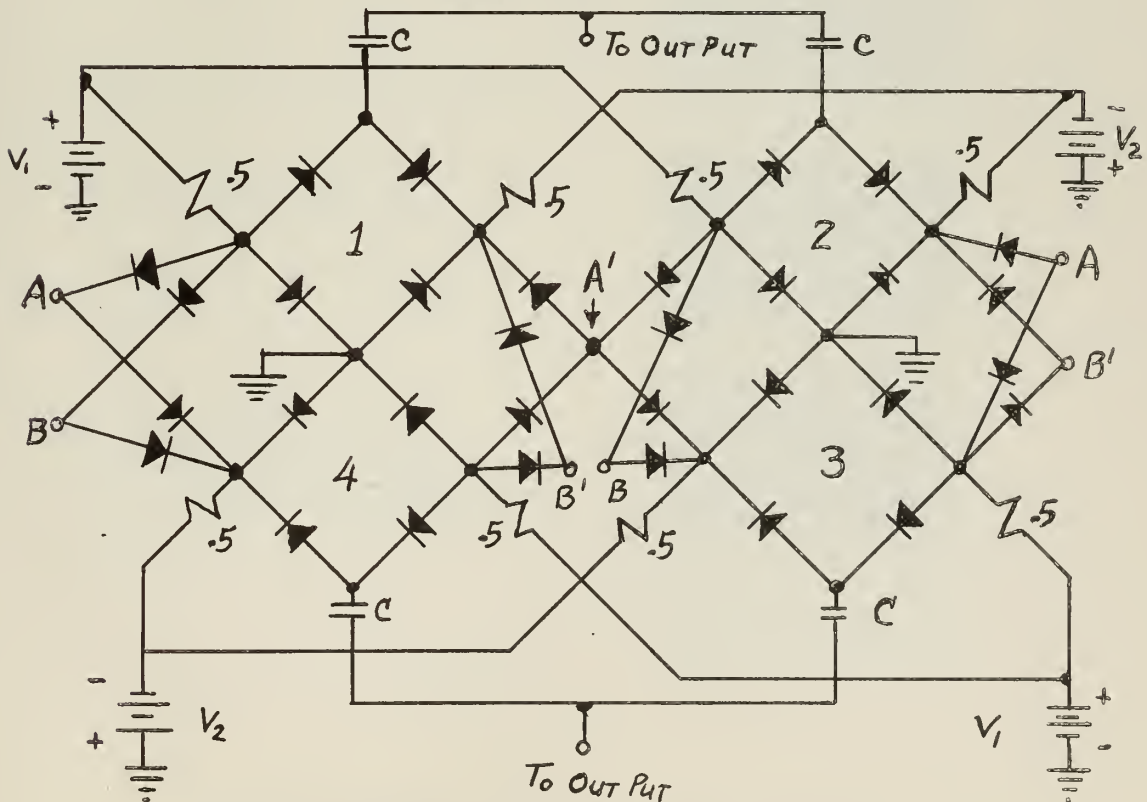
All diodes computer type
germanium similar to
1N68.

1 isol ampl'r ea for
A, A', B & B'
(A shown)



TYPICAL ISOLATION AMPL'R WITH SWITCH

Fig. (B-5)

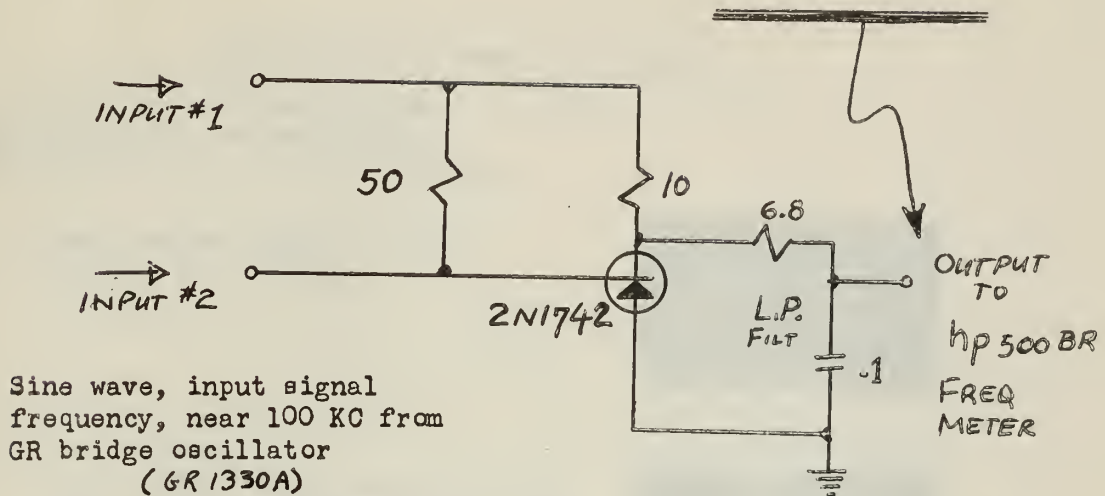


OVER-ALL CONNECTION SCHEMATIC FOR BRIDGES

Fig. (B-6)

Square wave from
B @ 100 KC (exactly)

Output is approx. a sine wave,
is the diff. freq. between
#1 & #2.



Sine wave, input signal
frequency, near 100 KC from
GR bridge oscillator
(GR 1330A)

OUTPUT
TO
hp 500 BR
FREQ
METER

MIXER CIRCUIT USED TO MEASURE FREQUENCY RESPONSES NEAR RESONANT PEAKS

Fig. (B-7)

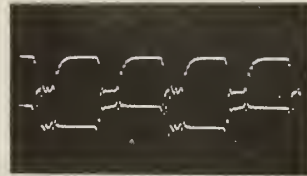
OSCILLOSCOPE WAVE FORMS AT $f_o = 250$ KC

All photos = 4 volts per division

(a) and (b) = $\frac{1}{2}$ sec per division

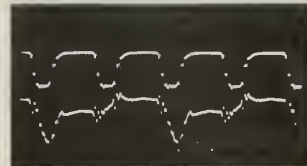
(c), (d) and (e) = 1 sec per division

(a) Top: SCHMITT trigger into gate
Bottom: "A" into gate



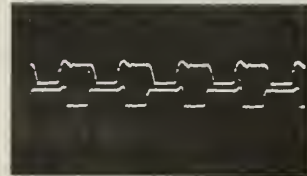
(a)

(b) Top: SCHMITT trigger into gate
Bottom: "AND" gate output into F.F.#2



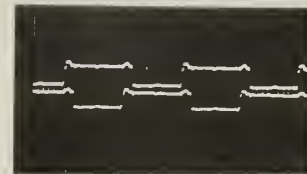
(b)

(c) Top: A' at diode modulators
Bottom: A at diode modulators



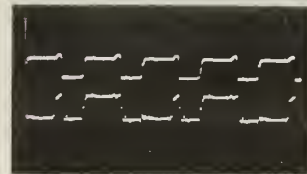
(c)

(d) Top: B at diode modulators
Bottom: B' at diode modulators



(d)

(e) Top: A at diode modulators
Bottom: Switching wave form on modulator #3, showing spurious "Turn-on" pulse.



(e)

Fig. (B-8)

OSCILLOSCOPE WAVE FORM PICTURES

(b) AND (c): $f_c = 100$ KC; ALL OTHERS: $f_c = 250$ KC

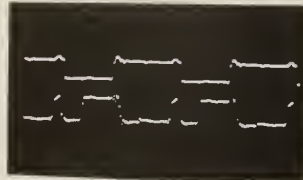
Photo Scales:

Time: (d) and (e) = $\frac{1}{2}$ sec per division
 (a) = 1 sec per division
 (b) and (c) = 2 sec per division

Amplitude:

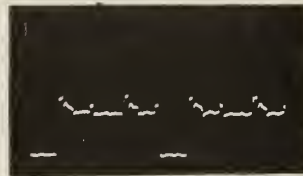
(b), (c) and (e) = $\frac{1}{2}$ volt per division
 (a) = 1 volt per division
 (d) = 2 volt per division

(a) Top: B at diode modulators
 Bottom: Switching wave form on modulator #3 showing spurious "turn-on" pulse (compare with Fig. (B-9)(e)).



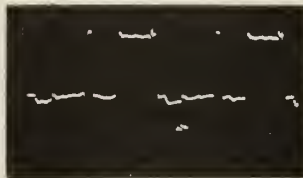
(a)

(b) Adjustment of diode modulator #3 with positive battery () bottom of picture is ground potential.



(b)

(c) Adjustment of diode modulator #3 with negative battery (-) top of picture is ground potential.



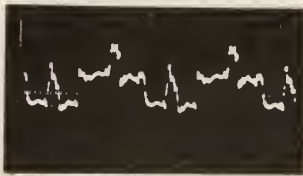
(c)

(d) View of 250 KC signal output near resonant point, showing spurious noise pulses.



(d)

(e) 250 KC signal output with switch exactly synchronized with input signal. Note noise pulses.



(e)

Fig. (B-9)

thesS4372

Investigations of a tunable radio freque



3 2768 001 94386 3

DUDLEY KNOX LIBRARY